MEASUREMENT OF RESIN PRESSURE IN COMPOSITE LAMINATES DURING CURE

by

KATHERINE ANN MACKENZIE

B.A.Sc., The University of Waterloo, 1990

A THESIS SUBMITTED IN PARTIAL FULFILLMENT OF

THE REQUIREMENTS FOR THE DEGREE OF

MASTER OF APPLIED SCIENCE

in

THE FACULTY OF GRADUATE STUDIES

Department of Metals and Materials Engineering

We accept this thesis as conforming

to the required standard

THE UNIVERSITY OF BRITISH COLUMBIA

April 1993

In presenting this thesis in partial fulfilment of the requirements for an advanced degree at the University of British Columbia, I agree that the Library shall make it freely available for reference and study. I further agree that permission for extensive copying of this thesis for scholarly purposes may be granted by the head of my department or by his or her representatives. It is understood that copying or publication of this thesis for financial gain shall not be allowed without my written permission.

(Signature) _____

Department of Metals and Materials Engineering

The University of British Columbia
Vancouver, Canada

Date April 23/93

Abstract

A promising method of measuring the resin pressure within a composite laminate during processing has been developed. This method can be used to investigate the control of voids, or resin flow and laminate compaction in several composite material processing methods such as AC/VD, hot press curing and resin transfer moulding.

Sensor assemblies were developed and tested to show that their response is reproducible, linear and stable with temperature and time. Resin pressure profiles for three AS4/3501-6 laminates were generated and compared.

The experimental results were compared to a resin flow model simulation. The prepreg used for the experiments was aged, so the simulation was run several times with various initial degrees of cure of the resin. Experimental data were compared to the simulation predictions to determine the apparent initial degree of cure of the resin, and the resin pressure profiles from the experiments and the simulation with this resin initial degree of cure were compared.

The resin pressure within a laminate increases with the applied pressure until flow begins, at which time the resin pressure drops off progressively through the laminate thickness from the top surface to the toolplate. Conversely, the pressure at the surface of the laminate, next to the bleeder, remains at the vacuum pressure until the onset of flow when it increases as resin enters the bleeder. The measured resin pressure profiles were consistent both with the experimental results, and the simulation predictions. An advanced degree of cure of the resin at the start of the cure cycle significantly affects the resin flow and compaction in a laminate during cure.

Sommaire

Une nouvelle méthode expérimentale est développée permettant de mesurer la pression hydrostatique de la résine à l'intérieur d'un composite laminé durant sa fabrication. Cette méthode permet d'évaluer entre autre l'écoulement de la résine, la compaction du laminé et la formation de porosités. Elle peut être employée dans plusieurs procédés de fabrication des matériaux composites: le moulage par compression, le moulage sous vide en autoclave ou le moulage par injection de résine.

Des capteurs composés d'un tube capillaire rempli de résine sans durcisseur relié à un capteur de pression sont développés et calibrés. Ces capteurs sont fiables, linéaires et insensibles à la température. La variation de la pression de résine est mesurée pour trois laminés formés d'un pré-imprégné AS4/3501-6.

Les résultats expérimentaux sont comparés avec ceux obtenus grâce à un programme simulant l'écoulement de la résine. Le pré-imprégné utilisé étant périmé, plusieurs simulations sont réalisées pour différents degrés initiaux de polymérisation de la résine.

La pression de la résine dans le laminé augmente proportionnellement avec la pression externe appliquée jusqu'à ce que la résine commence à s'écouler. A ce moment, la pression de la résine diminue progressivement depuis la surface supérieure du laminé vers la surface du moule. Inversement, la pression au niveau du feutre reste à la pression du vide jusqu'à ce que la resine s'écoule dans le feutre provoquant une augmentation de la pression. Les gradients de pression mesurés confirment les autres observations expérimentales et les prédictions des simulations. Enfin, le degré initial de polymérisation de la résine a un effet important sur l'écoulement de la résine et la compaction du laminé durant sa polymérisation.

Table of Contents

Abstract ii

Sommaire iii

Table of Figures vii

Table of Tables ix

Acknowledgments x

Chapter 1: Introduction 1

1.1. Motivation and Goals of this Work 1

1.2. Material System and Process Route 2

1.3. Scope and Organization of This Work 4

1.4. Figures 6

Chapter 2: Literature Review 7

2.1. Experimental Work 7

2.2. Models 10

Chapter 3: Development of Pressure Sensors 14

3.1. Principle 14

3.2. Construction and Application 15

3.3. Verification of the Sensor Response 16

3.3. Figures 20

Chapter 4: Experiments 24

4.1. General 24

4.2. Laminate Run A 25

4.3. Laminate Run B 29

4.4. Laminate Run C 33

4.5. Post-Gelation Behaviour 35
4.6. Figures 38
Chapter 5: Comparison With Model Results 45
5.1. Determination of the Apparent Initial Degree of Cure of the Resin 47
5.1.1. Resin Pressure 49
5.1.2. Resin Loss 52
5.1.3. Laminate Compaction 54
5.1.4. Summary 55
5.2. Comparison of Experimental Resin Pressure Profiles With Simulation Results for α_i = 0.35 - 0.40. 56
5.3. Figures 58
Chapter 6: Conclusions and Recommendations 63
6.1. Conclusions 63
6.2. Recommendations 64
References 67
Appendix A: Displacement of the Tube Walls Due to Process Conditions 70
A.1. Hydrostatic Pressure 70
A.2. Vertical Squeezing Pressure 71
Appendix B: SenSym SCC100A Specifications 72
B.1. Pressure Sensor Characteristics 72
B.2. Performance Characteristics 72
Appendix C: Nitric Acid Digestion of Laminates 74
Appendix D: Nitric Acid Digestion of Prepreg 76
Appendix E: Input File For LamCure Simulations 79
Appendix F: Acetone Digestion of Prepreg 87
Appendix G: Conversion of Resin Height in the Bleeder to Resin Mass 90

Appendix H: Resin Mass Lost from Laminates A and C 91

H.1. Bleeder Masses 91

H.2. Mass Change per Area 92

H.3. Checking the Mass Change per Area Results With the Measured Laminate and Prepreg M_f Results 93

H.4. Comparison of Bleeder Mass and Mass Change per Area Results 94

Table of Figures

Figure 3-1. Schematic of the tube sensor assembly. 20
Figure 3-2. Typical sensor response to pressure at room temperature. 20
Figure 3-3. Pressurization results for four sensors..... 21
Figure 3-4. Typical sensor response to temperature and time..... 21
Figure 3-5. Typical sensor response to pressure at 26°C and 80°C..... 22
Figure 3-6. Comparison of sensor response before and after Laminate Run A..... 22
Figure 3-7. Verification of the sensors as absolute devices..... 23
Figure 4-1. Laminate Run A vacuum bag assembly. 38
Figure 4-2. Placement of sensor tubes in Laminate Run A..... 38
Figure 4-3. Cure cycle for Laminate Run A..... 39
Figure 4-4. Resin pressure throughout the cure cycle for Laminate Run A. 39
Figure 4-5. Resin pressure over the first 100 min. of cure cycle for Laminate Run A..... 40
Figure 4-6. Two calibration curves for Sensor #5..... 40
Figure 4-7. Cure cycle for Laminate Run B..... 41
Figure 4-8. Resin pressure over the first 70 min. of cure cycle for Laminate Run B..... 41
Figure 4-9. Resin pressure over the first 24 min. of cure cycle for Laminate Run B..... 42
Figure 4-10. Resin Pressures at 105, 115, and 125 min. after pressure application for Laminate Runs A, B and C..... 42
Figure 4-11. Cure cycle for Laminate Run C..... 43
Figure 4-12. Resin pressure throughout the cure cycle for Laminate Run C. 43

Figure 4-13. Resin pressure over the first 100 min. of cure cycle for Laminate Run C. 44
Figure 5-1. Laminate Run A - Simulation prediction for 0 initial degree of cure. 58
Figure 5-2. Laminate Run A - Simulation prediction for 0.15 initial degree of cure. 59
Figure 5-3. Laminate Run A - Simulation prediction for 0.25 initial degree of cure. 59
Figure 5-4. Laminate Run A - Simulation prediction for 0.35 initial degree of cure. 60
Figure 5-5. Laminate Run A - Simulation prediction for 0.40 initial degree of cure. 60
Figure 5-6. Laminate Run A - Simulation prediction for 0.45 initial degree of cure. 61
Figure 5-7. Laminate Run A - Simulation predictions of the resin viscosity profile.. 61
Figure 5-8. Laminate Run A - Simulation predictions of laminate compaction over the cure cycle. 62
Figure 5-9. Laminate Run A - Simulation predictions of the final volume fraction of fibres. 62
Figure 5-10. Resin pressure at the 1/2 point for simulations and Laminate A..... 63

Table of Tables

Table 3-1. Comparison of calibration curves for several sensors. 18

Table 4-1. Sensor reactions to known vacuum losses, shown in Figure 4-9. 32

Table 5-1. Magnitude and timing of resin pressure drops in simulated and real laminates. 51

Table 5-2. Simulation predictions of the amount of resin flow into the bleeder for various prepreg initial degrees of cure. 52

Table 5-3. Final resin mass loss values of simulated and real laminates 53

Table 5-4. Comparison of final average volume fraction of fibres for simulated laminates to results of nitric acid digestion of real laminates 54

Table 5-5. Summary of experimental and simulation results. 56

Acknowledgments

Throughout the development of this thesis, there were many people whose contributions cannot be ignored and whom I wish to thank for their ideas, knowledge and arguments, as well as their friendship. I would like to thank Dr. Anoush Poursartip for his guidance, enthusiasm and interest in this work. I thank the Cy and Emerald Keyes Foundation for the fellowship which supported part of this work. Greg Smith and Golnar Riahi each shared with me a wealth of processing information and experience, and I thank them for their knowledge and assistance. I am grateful to Dennis Chinatambi, Pascal Hubert and Andrew Johnston for their invaluable assistance and ideas, and Brian Coxon of *intec* for his suggestions. For their help with design, manufacture and wiring, and the use of the production equipment, I thank Roger Bennett, Serge Milaire, Ross McLeod, Carl Ng and Ed Armstrong. I would also like to express my gratitude to Reza Vaziri, Daniel Delfosse, Mary Mager, Scott Ferguson, Isabelle Paris, and Mike Pierson for their useful discussions and other viewpoints, and for letting me use the computer. I would like to thank my family for their love and encouragement, and Chris Lynch for his patience and understanding and for helping me keep my sense of humour.

Chapter 1: Introduction

1.1. Motivation and Goals of this Work

Although composites have been produced industrially since the 1960's, many processes used in their manufacture are not well understood. Cure cycles developed by trial and error are used with the application of temperature and pressure designed to produce large process windows that accommodate differences in material condition and part geometries. Since these process cycles are not optimized for each different run, they may often be longer than required. Furthermore, improper curing can result in components which are poorly consolidated, contain voids and have unacceptable surface quality and physical properties. Since improperly cured composites cannot be recycled, they must be discarded.

The quality of a composite part is determined by the temperature and the pressure distribution in the part as it cures. The temperature controls how the crosslinking reaction of the thermoset matrix proceeds, while the pressure distribution drives the flow of the resin within and out of the composite. The effects of temperature on laminates has been fairly well characterized, but much is unknown about both the resin pressure distribution within a laminate during cure, and how this distribution affects the final properties of the composite. Ideally, at some point in the future, a computer model or expert system will be available to composite manufacturers which will produce a cure cycle for good quality parts with only the material specifications, the part geometry and fibre orientation requirements, and the capabilities of the processing equipment. The

ability to analyse and correct for unexpected events (for example a short power failure) would also be desirable.

Presently processing problems are encountered with uncontrolled resin flow and voids, especially in complex parts which may include corners, stiffening ribs, or honeycomb inserts. The ability to measure the resin pressure inside the laminate at these points would be extremely useful in identifying and solving these problems, reducing the number of discarded parts.

Increased knowledge of laminate processing in general shortens the trial and error process of determining cure cycles for new parts and enables cure cycles to be optimized to produce a good quality laminate in the shortest amount of time. Specific measurements of parameters indicative of flow, such as laminate resin pressure profiles and mass loss, are useful for the validation of process models.

There are two main goals of this work. The first is to develop a new pressure sensing device for measuring resin pressure within a laminate. The second goal is to use this device to investigate the resin pressure distribution in composite laminates during cure.

1.2. Material System and Process Route

The material used in this work is Hercules AS4/3501-6 carbon fibre reinforced epoxy. AS4/3501-6 is a well established, first generation material system and was chosen for this work because of both its widespread use, and the previous experimental results available. This material was received as a roll of unidirectional "prepreg" (a thin sheet of fibres and partially cured epoxy resin).

The autoclave vacuum degassing (AC/VD) process is the most commonly used process for producing composite parts for the aircraft/aerospace industry. This process involves cutting pieces of prepreg, and stacking them together on a toolplate such that the desired fibre orientations are achieved. The toolplate may be flat, or contoured to a complex geometry required of the final part. A typical layup is shown schematically in Figure 1-1.

For a "bleed" system, layers of absorbent cloth (bleeder layers) are laid on top of the laminate to absorb excess resin from the laminate during cure. Previously, composites were commonly processed in this way because it was difficult and costly to make prepreg with the high volume fraction of fibres required of the cured laminate. Currently, now that the prepregging technology has improved, these bleeder layers are often omitted resulting in a "no bleed" or "zero bleed" system, where the laminate contains the desired resin content from the start. The zero bleed method has the advantages, when compared to a bleed method, of wasting less material and requiring less time in the cure cycle for resin flow. Less flow of resin through the fibres results in less movement of the fibres and the outer surface of the part [1], therefore the quality of the final part should also be better for a zero bleed system.

A caul plate may be used to evenly distribute the pressure on the laminate, and dams may be placed around the edges of the laminate to prevent resin loss due to horizontal resin flow.

This assembly is covered with "breather" cloth and a plastic vacuum bag sealed to the toolplate with vacuum bag sealant tape. The breather layers ensure that the vacuum drawn on the bag reaches all areas of the assembly. The vacuum within the bag is

necessary to provide a pressure gradient across the laminate thickness to cause compaction. It also removes entrapped gases and volatiles from the laminate.

The completed assembly is placed in an autoclave, the vacuum bag is evacuated and the laminate is cured and consolidated by a "cure cycle" of increased pressure and temperature in a prescribed sequence over time. The increased temperature causes the thermoset matrix to crosslink, while the application of pressure forces the individual laminae together, causing the constituent fibres and resin to consolidate and flow together to create a single monolithic part.

1.3. Scope and Organization of This Work

In this thesis, the resin pressure distribution in composite laminates is investigated through the use of embedded resin pressure sensors in flat, cross-plied laminates cured by the AC/VD process.

This information is presented in the following chapters, with the figures contained in the last section of each.

The second chapter, **Literature Survey**, discusses the relevant literature important to clarify the goals and scope of this work.

In the third chapter, **Development of Pressure Sensors**, the resin pressure sensor assemblies developed here are described and the verification of the sensor responses discussed.

The fourth chapter, **Experiments**, describes the experimental work, in which the sensors were embedded in three composite laminates. The sensor responses throughout the cure process are presented and interpreted.

The sensor resin pressure results are compared to model results in the fifth chapter, **Comparison With Model Results**. A flow simulation correctly predicts the trend of the resin pressure distribution seen in the experiments presented in the previous chapter. Material parameters input to the simulation are adjusted to more closely match the experimental results, and the significance of these changes is discussed. Several experimental methods are used to compare the measured amount of resin flow out of the laminate to that predicted by the simulation.

In **Chapter 6**, conclusions are drawn and recommendations for further work are suggested.

1.4. Figures

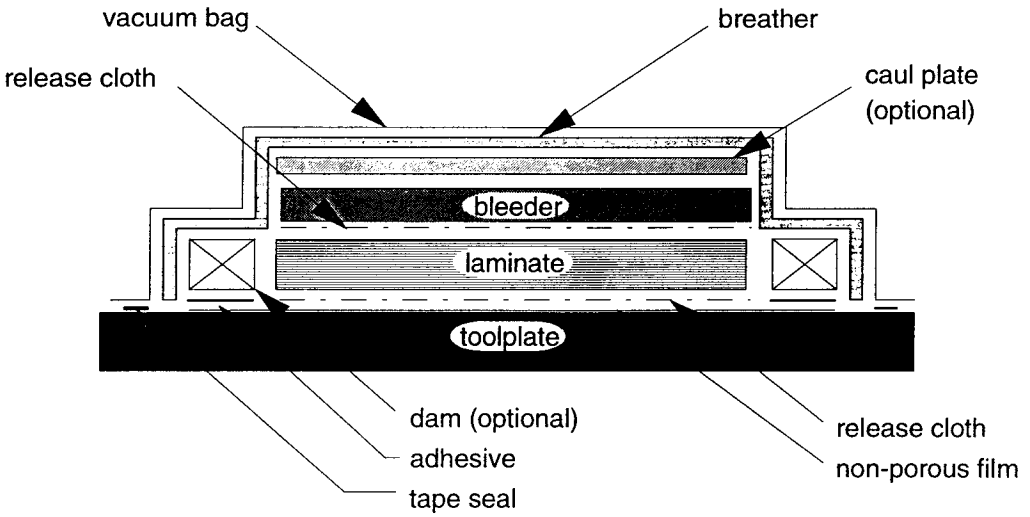

Figure 1-1. Schematic of a typical composite layup.

Chapter 2: Literature Review

2.1. Experimental Work

Determining the flow behaviour in composite laminates is a difficult task. The scale of fibres and resin is small (with dimensions of the order of 10 μm), the fibres are not ideally placed in uniform ranks, and the flow is affected by numerous factors including temperature, heating rate, and pressure difference. In the AC/VD process this study is further complicated since resin flows both parallel and perpendicular to the toolplate. Several methods have been used to try to understand and measure fluid flow in composite laminates. To date, no method has been entirely satisfactory.

Most commonly, researchers investigating resin flow in composites have relied on mass measurements of bleeder layers before and after the cure cycle [2-4]. Both top bleeders and side bleeders may be used [2] to measure flow perpendicular and parallel to the toolplate, singly or in tandem.

In order to determine when flow occurs, the cure cycle is interrupted at various times and the bleeder(s) weighed to determine the amount of resin gained by the bleeder (and therefore lost by the laminate) up to the time of interruption. This bleeder mass method is quite easily done and is useful for verifying model results. However it does not give any insight into the process of resin flow in a composite laminate. The source of the expelled resin, and the flow path are unknown.

Skartsis et al. [5] studied the flow of distilled water and silicone oil through ideal cylinder beds, and sheets of aligned carbon fibres, in different stacking sequences. The

measured permeabilities for various pressure differences across the carbon fibre "laminates" showed significant deviations from the results of tests with ideal cylinder beds. The choice of fluid also affected the results. The fibres in this study were held in their positions, and not allowed to rearrange during compaction. In addition, the fluid did not have the changing viscosity characteristics of a curing resin. These results are useful for validating models of flow through fibres and furthering the understanding of the permeability of composite fibre beds.

A method which illustrates flow within a laminate, even for zero-bleed systems, was developed by Poursartip et al. [6-8]. In this technique, prepreg is created with resin which has been "tagged" with bromine. That is, bromine atoms have been chemically attached to the molecules of the epoxy resin. Several plies of this prepreg are then laid up inside a laminate of untagged prepreg, and the assembly cured normally. After cure, the laminate is sectioned, and, by WDX (wavelength dispersive X-ray) analysis on a scanning electron microscope, the placement of the bromine atoms is traced creating a contour map of the brominated resin after cure. The placement of the brominated resin prior to cure is known, so comparing this to the final bromine distribution yields the amount and path(s) of resin flow. This technique provides both qualitative and quantitative results for resin flow, but is very time consuming and only gives the final results. The progression of the flow over time is not indicated.

A different approach to understanding the resin flow in a composite is to determine the resin pressure within the laminate. The pressure difference across the laminate is the driving force for resin flow and therefore fundamental to its understanding. The absolute resin pressure at any point in the laminate is also vital to the study and control of voids.

Measuring pressure in a laminate is difficult, mainly due to the size requirements [9]. Typically a carbon/epoxy lamina is approximately 0.125 mm thick. Thus any sensor placed inside the laminate must be very small so as not to excessively disturb the resin flow that the sensor is meant to investigate.

Smith [10] attempted to measure the resin pressure within composite laminates with flat, postage stamp-sized (0.34mm x 15mm x 20mm) sensors from Interlink Electronics of Santa Barbara, California. These are resistive sensors with interdigitated conductive fingers which are forced against a semi-conductive material by the applied pressure. The greater the applied pressure, the lower the resistance measured across the sensor. Results from three carbon fibre/epoxy laminates were presented. The sensors were inserted at the upper and lower surfaces of the laminates and 1/4, 1/2 and 3/4 of the way through the laminate thickness.

Several problems were found with these flat sensors. The polymeric substrate under the semi-conductive layer appeared to creep, especially at high temperatures, and the sensors displayed time-dependent, hysteritic responses to pressurization and depressurization. Also, the sensor responses were very noisy, and there was a large variation in response from sensor to sensor.

There is uncertainty as to what these sensors measure. These sensors cover a relatively large area in the plane of the composite, so some of the decrease in resistance measured could be due to fibres contacting the sensors. If the fibres are pressing against the sensors, then these sensors would be measuring not only the hydrostatic resin pressure, but a combination of the fibre bed pressure and the resin hydrostatic pressure. In addition, there is a path from the outside to the interior of each sensor. When the sensors are laid up into the laminate the interior cavities are at

atmospheric pressure. On application of vacuum to the laminate, they may become evacuated. However, once they are in the laminate, especially after external pressure is applied and the temperature increases, the pressure inside the sensors becomes indeterminate.

These problems led Smith [10] to conclude that the flat sensors could be used only in a qualitative fashion. The sensors could indicate whether the pressure in an area of the laminate was increasing or decreasing at a particular time, by the change in resistance measured.

These results were further supported by results from a fourth laminate [11] with layup and instrumentation very similar to that of Reference [10], their laminate designated #3. The trend of the data, both in magnitude and time frame, was similar to that reported by Smith. The variability of the data was very high, with almost half of the embedded sensors reporting large, rapid fluctuations over much of the cure cycle. The results from this laminate supported Smith's earlier conclusions, but did not provide further insight into the process.

2.2. Models

Mathematical models of resin flow in composite laminates have been developed with various approaches ranging from lubrication theory to soil mechanics and with different simplifications and assumptions related to the resin flow and the shape and packing of the fibres.

Lindt [12, 13] started with ideal parallel rigid cylinders in a square array. The flow through the cylinders was determined by summing the squeezing flow between

cylinders approaching each other and the drag flow of the fluid moving past all of the cylinders. Lindt drew on lubrication theory in developing this model. The fibres do not come into contact with each other, and therefore carry no load. Skartsis [5] similarly investigated flow through ideal cylinder arrangements, with no contact between the cylinders.

Currently the most commonly used flow models are based on D'Arcy's Law:

$$V = -\frac{S}{\mu}\frac{dP}{dz} \tag{2.1}$$

where:

V = average linear velocity of the fluid,

S = permeability of the porous medium,

μ = Newtonian viscosity of the fluid,

dP = pressure difference in the velocity direction, and

dz = bed length considered.

The use of D'Arcy's Law is suitable for one-dimensional, low Reynold's number flow through a fully saturated porous medium [14]. Although this equation can be extended to three dimensional flow [15], this is unnecessary for flat laminates with edge dams in which flow occurs normal to the toolplate only.

The first of these models [3] combined the D'Arcy's law approach with an empirical layer-by-layer compaction sequence [16], and was presented by Loos and Springer in 1983.

In this model, the compaction of the laminate may be described as sequential. With the application of pressure, the top ply, next to the bleeder, is pushed down towards the second ply, as resin is squeezed out from between these plies. When the first ply approaches the second ply, the two move together towards the third ply, while the resin between the second and third plies is squeezed out through the compacted region into the bleeder. Thus the fibres are treated as layers of neutral buoyancy material suspended in the resin at regular intervals. As the resin is squeezed out from the top of the laminate into the bleeder, the fibre layers do not resist compaction in any way, nor bear any of the load applied to the laminate. The result of this view of compaction is that there is a pressure drop only across the plies in the compacted region. The rest of the laminate is at the applied pressure.

Loos and Springer decoupled the resin flow in the directions parallel and normal to the axis of the fibres in order to facilitate calculations. Flow normal to the toolplate was modelled as flow through a porous medium, by using D'Arcy's law. Resin flow parallel to the toolplate was characterized as viscous flow between two parallel plates. The physical situation was modelled as one channel per ply containing all of the excess resin for that lamina. The pressure at the centreline of each lamina was considered to be the same, and was estimated from a force balance applied along the boundaries of the channel. It was assumed that the pressure gradient along the laminae is linear. The total resin flow is then simply the sum of the resin flow in the normal and parallel directions, ensuring that mass is conserved.

The second major approach consists of adding to D'Arcy's law the effect of the fibre network, which acts as a spring resisting compaction [15, 17-20]. The most common of these models is that of Davé and coworkers [15, 17] based on the fibre consolidation experiments of Gutowski [18].

Davé et al. treated the compacting laminate as a porous consolidating bed of fibres, by using equations developed for the consolidation of water-saturated soil. According to this view, as the laminate is compacted, the interaction between fibres increases and the fibres take more and more of the applied load. Thus in this model, there is a resin pressure gradient throughout the entire laminate, until complete compaction occurs and the resin pressure drops to zero. Davé et al. used a differential equation developed for soil mechanics which governs three-dimensional flow within a consolidating porous bed within a given time interval, modified with the appropriate boundary and initial conditions. The resin pressure determined from this equation was then used in D'Arcy's law to determine the resin velocity at any point in the laminate, at any time during the processing cycle.

Thus, the main difference between these two models is that Loos and Springer considered the situation to be flow through a porous media, while Davé et al. considered it to be flow and consolidation of a porous media.

Smith [10] coded both the models of Loos and Springer [3] and Davé and coworkers [15, 17] into a computer model, LamCure. He named the different approaches the Sequential Compaction Model and the Squeezed Sponge Model, respectively. Smith compared these theories and evaluated them based on the results of LamCure for each case. It was demonstrated that the Sequential Compaction Model is a special case of the Squeezed Sponge Model [10, 21] and Smith concluded that the Squeezed Sponge Model is a more realistic description of the flow in composite laminates.

Chapter 3: Development of Pressure Sensors

3.1. Principle

Measuring the pressure in composite laminates has proven to be a challenge, mainly because of the physical nature of the laminate [9]. A typical lamina is about 0.125 mm thick. Therefore a pressure sensing device should be close to this size in order to minimize its impact on the conditions that it is trying to report. In addition, a laminate contains both solid elements, the fibres, and a surrounding fluid, the resin. Thus, previously there has been problems determining what an embedded sensor is measuring: the fibre bed pressure, the resin hydrostatic pressure, or a combination of both [10].

The operation of the sensor assemblies described in this work is similar in principle to a static pressure tap. A small fluid-filled tube extends into the composite laminate. The hydrostatic pressure at the tip of the tube is transmitted by the fluid inside to a sensor mounted in contact with this fluid, outside the laminate.

There are two main benefits of this type of sensor. The first is the sensor's ability to measure only the resin hydrostatic pressure, and the second is the size and shape of the sensor assembly. The end of the tube is cut at ninety degrees to the applied force on the laminate. This means that, as long as the tube does not deform, the only pressure which can be transmitted to the sensor is the hydrostatic resin pressure, since it acts in all directions. Before gelation of the resin in the composite, deformation of the tube will also not affect the sensor reading, because the fluid will simply flow out the

end of the tube into the laminate. In any case, Appendix A contains calculations which show that deformation of the tubing under AC/VD conditions is negligible. The physical nature of the sensor assembly is beneficial because the long, thin shape of the tube is very unobtrusive to the flow within the laminate. Tubes are available with outside diameters as small as 0.2 mm (33 gauge). These tubes would easily fit within two layers of a typical composite laminate.

Having the sensor outside the laminate, and outside the vacuum bag, provides additional advantages. The environment of the sensor is then that of the autoclave, with elevated temperature and pressure the only concerns. This allows simpler and therefore less expensive sensors to be used, and also enables the sensors to be reused for many tests by simply replacing the tubing. Maintaining the seal of the vacuum bag is also simplified because the stainless steel tubes now penetrate the bag, rather than the PTFE coated wiring.

3.2. Construction and Application

The elements of the tube sensor include a tube, reservoir, plug and a pressure sensing device. A schematic of the assembly is shown in Figure 3-1.

The reservoir is a high pressure autoclave T-fitting, and the plug was manufactured in-house for these sensors. The plug, shown in Figure 3-1, contains an inner screw. This inner screw allows the volume of the reservoir to be decreased easily, after the sensor assembly has been filled. The tubing is 1 mm O.D. (19 gauge) needle tubing with a ninety degree tip, purchased from Chromatographic Specialties Inc. The tubing is attached to the reservoir by a gland nut with a ferrule providing the seal.

The pressure sensing device used is a SenSym SC100A absolute pressure sensor. These are diaphragm sensors, which function as Wheatstone bridges. They come packaged in a chip carrier, with a four-pin electrical connection. These sensors were chosen because they are inexpensive, and reported very good thermal stability and linearity. The manufacturer states that to achieve thermal stability, a constant current source is required. The datalogger used for this work, a Solartron/Schlumberger Orion Delta Datalogger, model 3530D, provides a constant voltage source for full bridge circuits. The sensors were therefore connected as resistors, energized by a constant current of 1 mA and produced output in Ohms. The manufacturers specifications for the pressure sensors are shown in Appendix B.

For use in a laminate, the sensor assembly is filled with fluid which will transmit the pressure at the tip of the tube to the sensor diaphragm. Uncatalysed epoxy resin was used for the fluid, since its similar composition should reduce the risk of incompatibilities such as chemical reactions and non-wetting between the sensor fluid and the laminate resin. Care is taken during filling to ensure that no air is left inside the sensor assemblies.

3.3. Verification of the Sensor Response

The response of the sensors, without the tube assemblies, was tested in several ways, before the sensors were used in composite laminates. The sensors were subjected to varying pressures at both room and high temperatures, and to constant pressure with varying temperatures.

A typical sensor's response to pressure at room temperature is shown in Figure 3-2. The pressurization and depressurization curves overlap closely, with negligible

hysteresis. Figure 3-3 shows pressurization results for several sensors. The results demonstrate that there is not much variation between sensors. Each sensor was calibrated separately to accurately obtain the relationship between resistance and pressure, although for the twenty sensors tested the slopes ranged only from 1.63 to 2.14, a variation of 0.51.

A test with a constant, 60 psig (414 000 Pa) pressure, and varying temperature produced the (typical) results in Figure 3-4. This figure shows that the sensors are stable with time, and that they respond minimally to changing temperature. This temperature insensitivity is further illustrated by Figure 3-5 which combines one sensor's responses to pressure ramps at both 26°C and 80°C. The sensor response is both linear and reproducible, despite the difference in testing temperatures.

This reproducibility was verified by retesting these sensors, after they were used in a laminate run, and had therefore been through an entire cure cycle. On comparing the results from this pressure cycle with the resistance curves from before the laminate run, (Figure 3-6), excellent agreement is obtained with a maximum difference for any sensor (shown in Figure 3-6) of 5 Ohms at 65 psig (448 000 Pa). This translates to 2.3 psi (16 000 Pa), or a 3.5 % variation.

This consistent linear behaviour made it possible to convert the resistance data to pressure for each sensor by the use of a simple, linear curve-fitting routine. Thus before a sensor was used, it was subjected to a pressure cycle and its calibration equation determined from a plot of resistance versus pressure. Table 3-1 shows the calibration curves for ten of the sensors. The equations are quite similar, demonstrating the lack of variation between the sensors. The form of the calibration equations is as follows:

$$y = mx + b \tag{3.1}$$

where:

y = resistance in Ohms

m = slope

x = applied pressure in psig

b = y-intercept

Sensor	Calibration Equation
#1	$y = 2.14x + 26.93$
#2	$y = 2.11x + 9.84$
#3	$y = 1.93x + 7.84$
#4	$y = 2.06x + 16.61$
#5	$y = 1.94x + 28.44$
#6	$y = 1.94x + 20.07$
#7	$y = 1.75x + 9.23$
#8	$y = 2.04x + 14.01$
#9	$y = 2.05x + 10.14$
#10	$y = 2.00x + 8.85$

Table 3-1. Comparison of calibration curves for several sensors.

In order to confirm that the sensors are absolute devices, unaffected by the autoclave pressure surrounding them, small caps were used to seal them, and they were subjected to a pressure cycle. The caps were simply nuts that had been placed into a pool of epoxy glue to seal off one end. These were then screwed onto the threaded portion of the sensor.

Typical results for a sealed and unsealed sensor are shown in Figure 3-7. The results confirm that the sensors are absolute devices.

Having shown that these sensors are non-hysteritic, reproducible, linear, and stable with time and temperature, these absolute pressure sensing devices were embedded in composite laminates, as described in the following chapter.

3.3. Figures

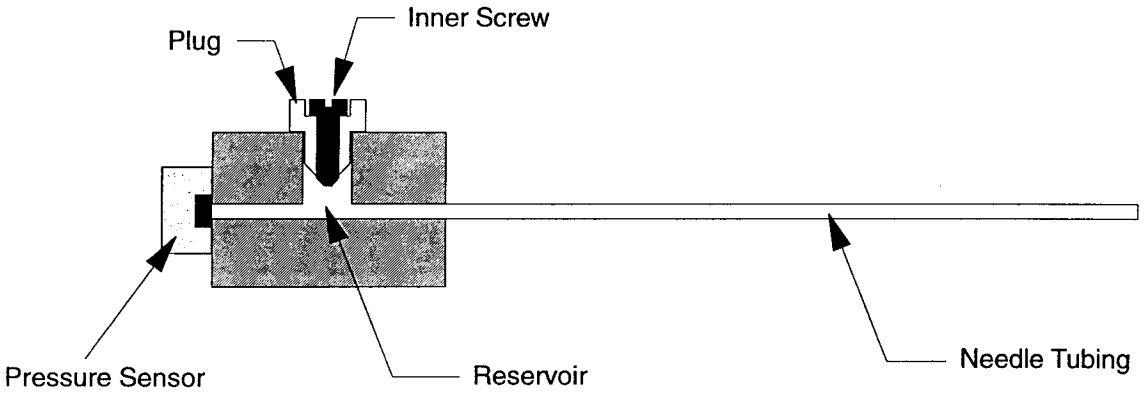

Figure 3-1. Schematic of the tube sensor assembly.

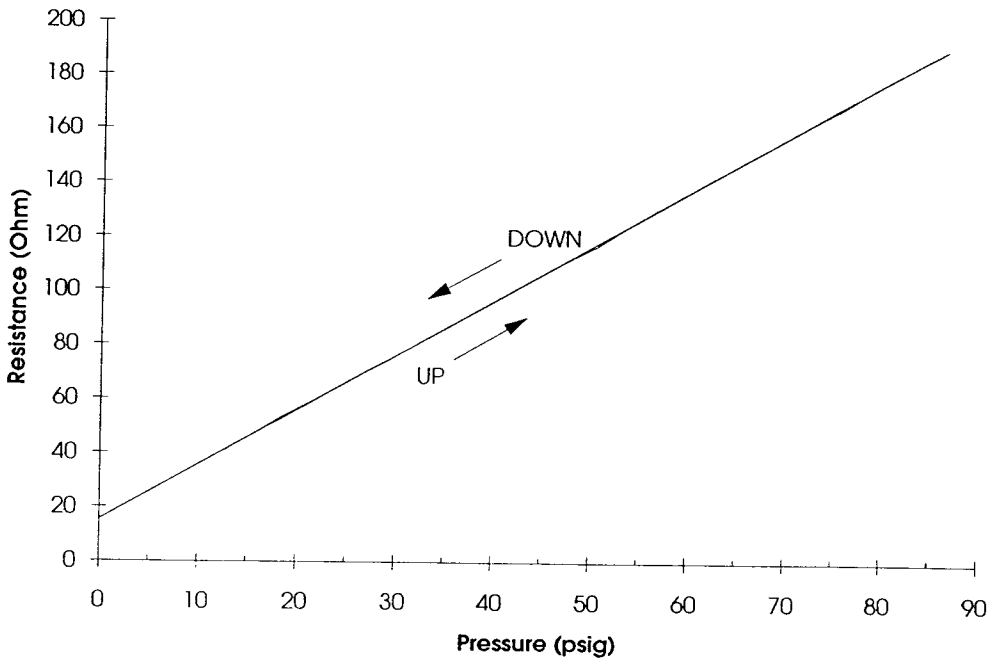

Figure 3-2. Typical sensor response to pressure at room temperature.

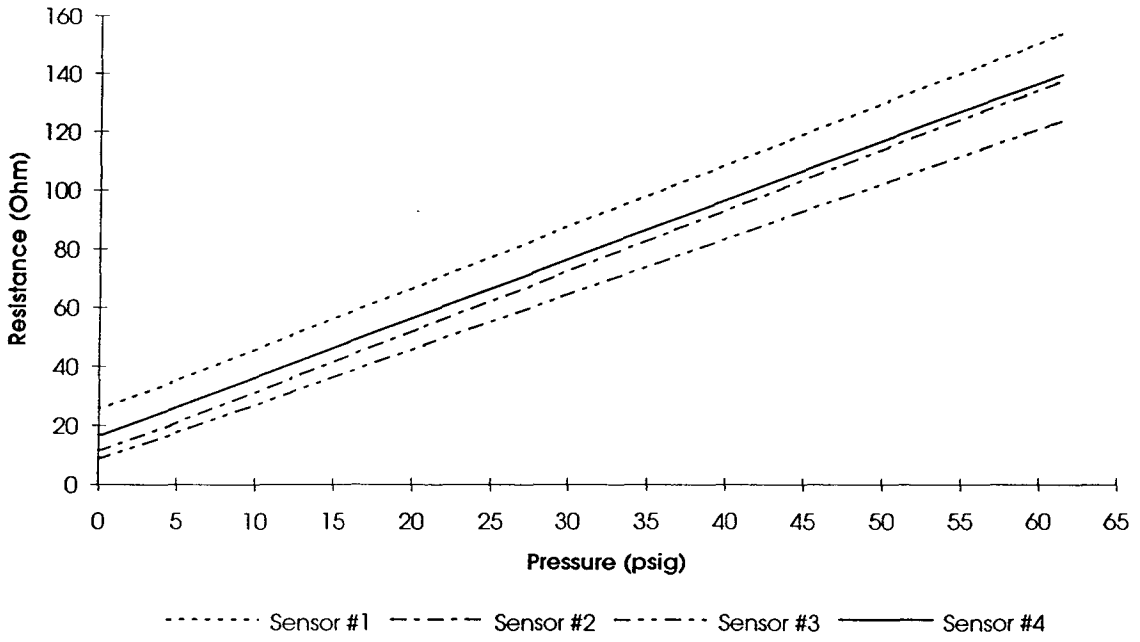

Figure 3-3. Pressurization results for four sensors.

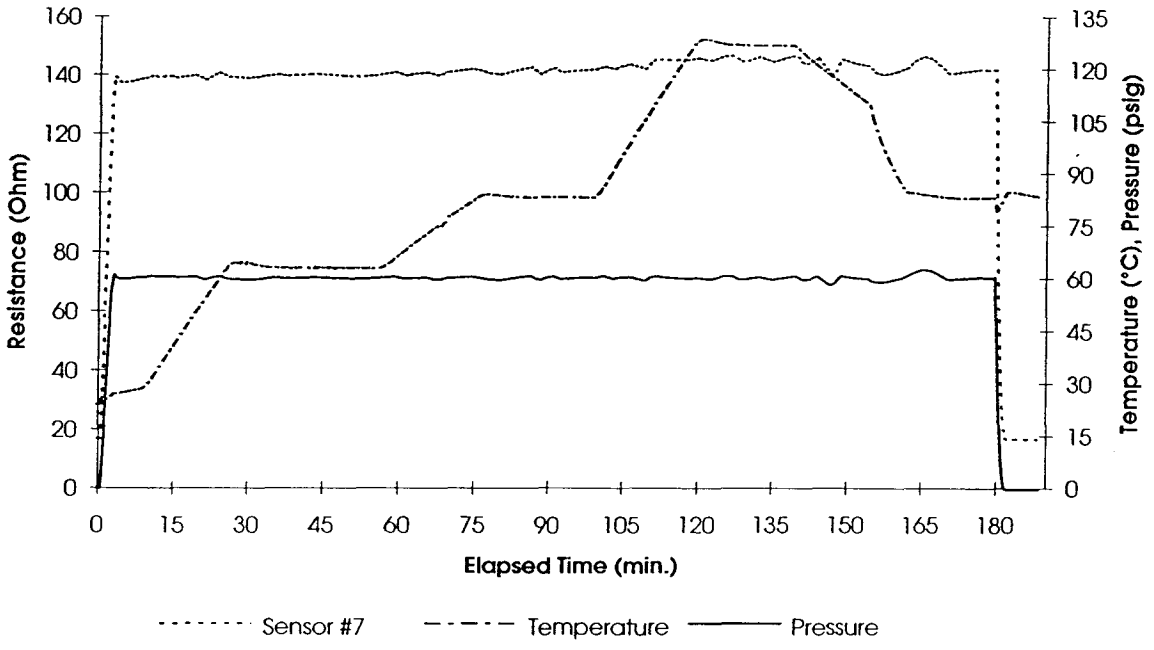

Figure 3-4. Typical sensor response to temperature and time.

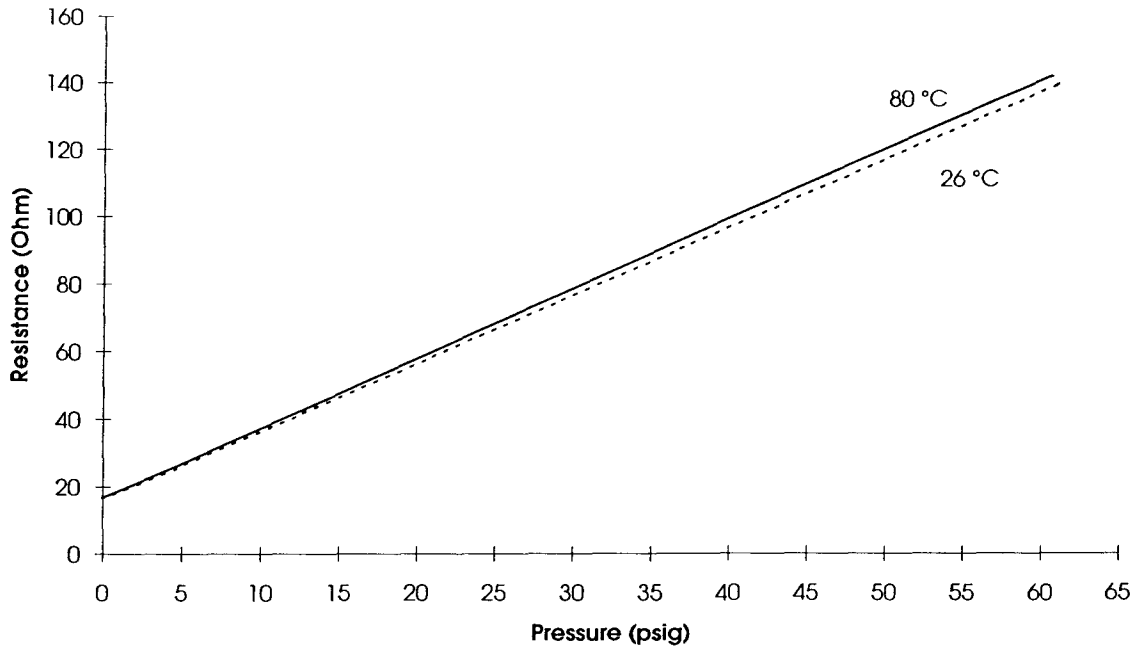

Figure 3-5. Typical sensor response to pressure at 26°C and 80°C.

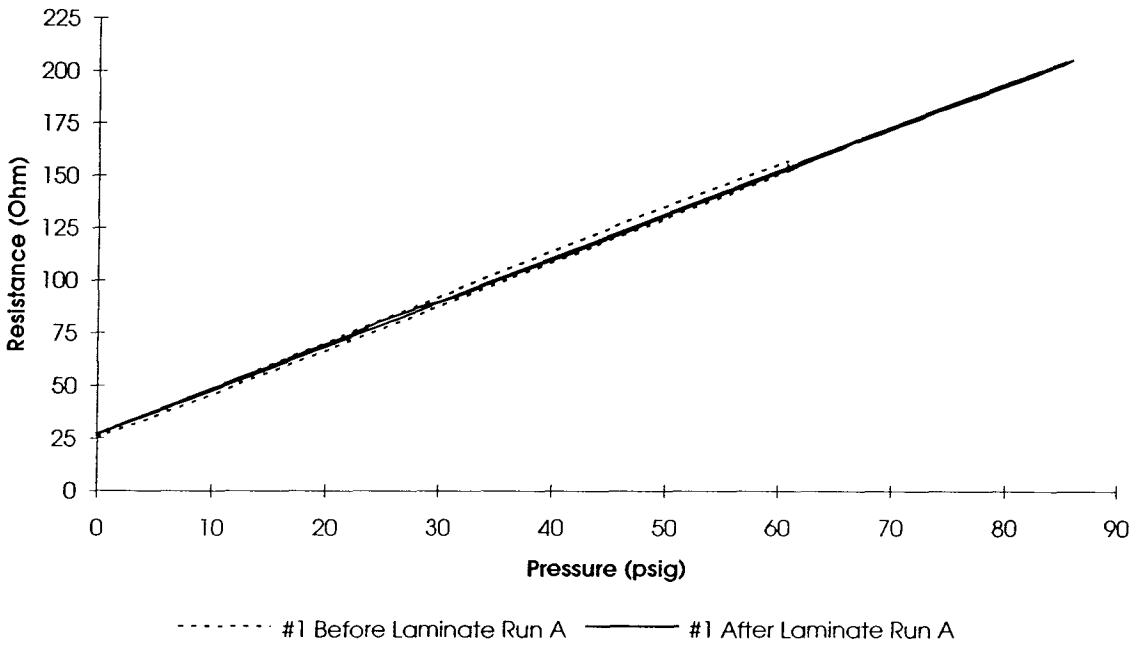

Figure 3-6. Comparison of sensor response before and after Laminate Run A.

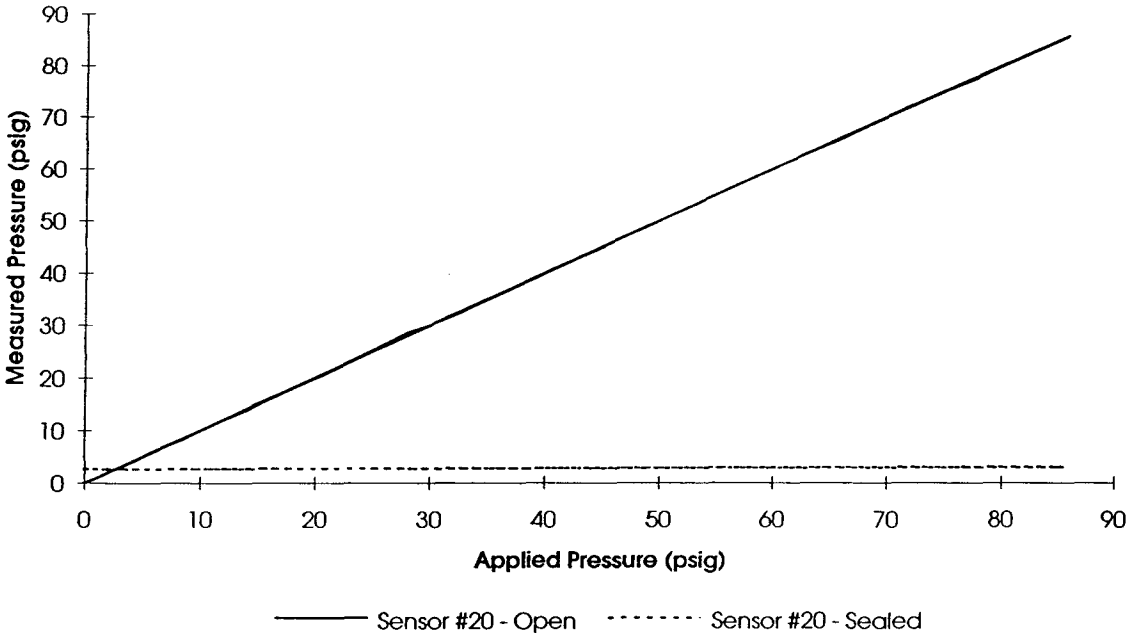

Figure 3-7. Verification of the sensors as absolute devices.

Chapter 4: Experiments

4.1. General

Three 10 cm by 10 cm, AS4/3501-6 carbon fibre reinforced epoxy laminates were instrumented with tube sensors. Each laminate was laid up as a bleed system, with layers of bleeder cloth placed on top of the laminate to absorb the excess resin during compaction. The laminates contained 48, 96, and 48 plies respectively and each had tube sensors positioned: at the interface between the bleeder and the top ply, 1/4, 1/2 and 3/4 through the laminate thickness, and between the bottom ply and the toolplate.

The layup for each laminate proceeded as follows: sets of two adjacent plies were rolled together, then vacuum degassed for two to five minutes. These ply couples were then rolled together to form four quarters of the laminate, less the ply couple just above a sensor. Thus the pieces formed for the 48 ply laminates contained plies numbered:

- 1, 2
- 3 - 12
- 13, 14
- 15 - 24
- 25, 26
- 27 - 36
- 37, 38
- 39 - 48

The layup was done in this manner so that the vacuum degassing had only to penetrate to a depth of two plies each time. Vacuum bag sealant was then used to dam the edges of each laminate, to prevent resin flow out of the laminate along the fibres, parallel to the plane of the toolplate.

The laminates were vacuum bagged with the sensor tubes extending through the vacuum bag, such that the actual sensors and their associated wiring all lay outside the vacuum bag. A photograph of the setup for Laminate Run A is shown in Figure 4-1. Indicated on the photograph are: (1) a tube sensor assembly, (2) a tube where it enters the vacuum bag, (3) the laminate covered by the bleeder plies and the vacuum bag, (4) the dam around the laminate, (5) the vacuum coupling, (6) the breather, under the vacuum bag, and (7) the vacuum bag sealant tape.

Each laminate assembly was then placed in an autoclave, evacuated, and subjected to pressure and temperature cycles, as described in the following sections.

4.2. Laminate Run A

The first test of the tube sensors in the AC/VD process was Laminate Run A, which produced a 48-ply $(0/90_2/0)_{12}$ laminate. This stacking sequence was chosen so that the tubes could be laid up between two plies with the same fibre orientation, thus minimizing the disturbance of the fibre compaction and resin flow.

The sensors were inserted:

- at the interface between the bleeder and the top ply of the laminate,
- between the 12th and 13th laminae (1/4 of the laminate thickness down from the bleeder),
- between the 24th and 25th laminae (1/2 way through the thickness of the laminate),
- between the 36th and 37th laminae (3/4 of the laminate thickness down from the bleeder), and
- between the toolplate and the bottom (48th) ply of the laminate.

To prevent any disturbance in the laminate from one sensor tube affecting the response of any other sensor, the tubes were laid up such that only one tube was in a given vertical line. As shown in Figure 4-2, the tubes were separated horizontally by at least 10 mm, and all of the tube ends were 6 mm from the centreline of the laminate. After cure, this laminate was sectioned, polished and inspected under an optical microscope. The distortion of the laminate around the sensor tube extended approximately 1 mm in all directions.

The laminate was laid up with thirty-six plies of bleeder cloth to absorb the excess resin from the laminate. Opening up the vacuum bag after cure showed that all thirty-six plies of the bleeder were almost saturated with resin. Clearly resin flow occurred during the cure cycle.

The cure cycle applied during Laminate Run A is shown in Figure 4-3. This cycle was used in order to facilitate comparison of the results to that of previous resin pressure experiments using flat sensors [10]. The pressure was released in steps at the end of this cycle in order to observe the response of the sensors to pressure in the cured laminate. For the same reason a rapid 50 psig (345 000 Pa) pressure spike was applied at the end of the cycle.

The experimental results from Laminate Run A are shown in Figure 4-4 and the first one hundred minutes are enlarged in Figure 4-5.

When the pressure in the autoclave is increased, all of the sensors, with the exception of the interface sensor, react by reading an increasing pressure with time. The time for a sensor to reach its highest pressure depends on where it is in the laminate, with the

toolplate sensor first, progressing in sequence then to the 3/4 point sensor, the 1/2 point sensor, and finally the 1/4 point sensor.

At approximately fifty minutes into the cure cycle, these sensors all show a drop in resin pressure. At the same time, the interface sensor shows an abrupt increase in resin pressure that corresponds to the decrease in the other sensors.

All of the sensors (including that at the interface) level off at about one hundred minutes and maintain their relative spacings for the duration of the test. The order of the sensors, with decreasing pressure, at any point in time is toolplate, 3/4 point, 1/2 point, 1/4 point, interface. Thus a pressure gradient is locked into the laminate until it cures.

It should be noted that the sensor assembly used at the toolplate position for this test was found to not produce a linear, reproducible result. This sensor was not calibrated prior to Laminate Run A, so two calibration pressure cycles were run for it, after the laminate run. In each of these tests, the autoclave pressure was ramped up to 30 psig (207 000 Pa), held for 8 minutes, ramped up to 85 psig (586 000 Pa), held for 10 minutes, ramped down to 30 psig (207 000 Pa), held for 8 minutes then gradually vented to atmospheric. Figure 4-6 shows the results; from this data it is not possible to know the correct calibration curve for the experiment. The calibration curve based on the results of the second test (Calibration Run 2) appears to give more reasonable values for Laminate Run A based on the initial and final conditions. At the beginning of Laminate Run A, before the application of pressure, the vacuum, as read from an external gauge, was at -14.8 psig (-700 Pa). At this same time, the toolplate sensor registers pressures of -16.2 psig (-10 400 Pa), if Calibration Run 1 were used, or -14.3 psig (2 700 Pa) if Calibration Run 2 were used. When the pressure and vacuum are released, at the end of Laminate Run A, the vacuum bag returns to atmospheric

pressure, 0 psig (101 325 Pa). The toolplate sensor at this time registers pressures of -5 psig (66 800 Pa) and -2 psig (87 500 Pa) using Calibration Run 1 and Calibration Run 2 respectively. Thus, both initially and finally, the results based on Calibration Run 2 are more consistent than those based on Calibration Run 1, and therefore it has been used.

The resin pressure distribution registered by the tube sensor assemblies shows that as the applied pressure increases, the entire laminate feels the pressure, although the sensor response is affected by the amount of settling done by the bleeder layers, and by the fibres and resin around each sensor. If for example, a sensor tube were inserted crookedly into the laminate, it could hold the fibres around it apart, resulting, initially, in a cavity at its tip which is not filled with resin. The interface sensor, because of its placement on the surface of the laminate next to the bleeder, does not have resin at its tip and reads the pressure in the bleeder, i.e. the vacuum pressure. At the start of the test the laminate behaves like a solid because the resin is too viscous to flow and therefore bears the pressure applied to it. The fibres are generally surrounded by resin, there is little contact between fibres, and so they bear little of the load.

After fifty minutes, the viscosity of the resin is low enough that it begins to flow. As the resin flows out from between the fibres, the fibres start to interact and take the applied load while the resin pressure drops. The resin moves up through the laminate, and into the bleeder, past the interface sensor. As the end of the interface sensor tube is covered by this resin, it begins to read a resin pressure as well.

The sensors all level off at about one hundred minutes, despite the fact that there remains a pressure gradient through the thickness of the laminate. Thus the resin has stopped flowing. This could be due to a combination of factors, such as the decrease in

the permeability of the fibre network due to compaction, coupled with the increase in resin viscosity due to the increased degree of cure of the resin. As the laminate compacts, the fibres are forced together. The spaces between the fibres get smaller as the fibre bed is compressed, making it more difficult for the resin to pass through. At the same time, the resin is continuously curing, and becoming increasingly viscous. At some point, the increasingly viscous resin can no longer be forced through the decreasingly permeable fibre bed by the pressure gradient across the laminate, and flow stops.

4.3. Laminate Run B

Laminate Run B created a 96 ply $(0/90_2/0)_{24}$ laminate. The purpose of making such a thick laminate was to magnify the effects of the resin pressure gradient through the laminate thickness. As before, the sensors were placed:

- at the laminate/bleeder interface,
- between the 24th and 25th laminae (1/4 point),
- between the 48th and 49th laminae (1/2 point),
- between the 72nd and 73rd laminae (3/4 point), and
- between the 96th lamina and the toolplate.

Three additional sensors were added:

- between the 24th and 25th bleeder plies (lower bleeder),
- between the 48th and 49th bleeder plies (mid bleeder), and
- between the 84th and 85th bleeder plies (upper bleeder).

In this thick laminate, thermocouples were placed in the centre of the laminate, and at the laminate/bleeder interface. The thermocouples were laid up perpendicular to the sensor tubes, 6 mm off the laminate centreline and with their ends 10 mm from the end of the tube at that level, to avoid interaction.

Laminate B was vacuum-bagged with 96 bleeder cloth layers to ensure excess bleeder volume. It was hoped that the upper bleeder sensor would never be reached by resin and therefore could be used as a comparison, or control.

The cure cycle, Figure 4-7, approximated the manufacturers recommended cure cycle. The pressure would normally be increased to 100 psig (689 000 Pa) at the second temperature ramp, but the autoclave used can only be safely pressurized to 90 psig (621 000 Pa) so this was the maximum pressure applied. The large fluctuations in temperature after 140 minutes were due to malfunctioning of the temperature controller which was supposed to hold the autoclave temperature at 177 C (350 °F) after this time.

Great difficulties were encountered in trying to draw a vacuum on this laminate. The vacuum bag held only until the pressure increased to approximately 20 psig (138 000 Pa), then opened up to the external autoclave pressure. The result of the lack of a sealed vacuum bag was that the system became a zero-bleed, zero-compaction system. Since the entire laminate was surrounded by the full autoclave pressure, there was no pressure gradient to cause resin flow, or compaction.

Despite these problems, some of the test results are still useful. The data for the (short) time period before and during the loss of the vacuum can be compared to the start of Laminate Run A. In addition, the sensor responses for a zero-flow system are now

known. The results for the first seventy minutes of Laminate Run B are shown in Figure 4-8, and the initial 24 minutes are expanded in Figure 4-9.

With the application of pressure, a similar response to that displayed in Laminate Run A is observed, until at approximately twelve minutes the independent, external vacuum gauge indicated that the vacuum bag had started to leak, and at twenty minutes opened up completely. Before the loss of the vacuum, however, the interface sensor pressure stayed low, while the other sensors showed increasing pressures: the toolplate, and 3/4 point sensor first, the 1/4 point sensor more slowly, as in Laminate Run A. No data is presented for the 1/2 point sensor as it gave faulty readings and ceased to function.

The times on Figure 4-9 marked "A", "B", and "C" refer to Table 4-1 below. This table shows the observed incremental loss of vacuum during the test, and describes the reaction of the sensors at these times.

As described in Table 4-1, at point "A", although there is no jump in the applied pressure, there is a noticeable increase in the responses of the 1/4 point, 3/4 point, and toolplate sensors. In addition, the mid bleeder sensor which did not respond to the applied pressure previously, starts to increase. A similar, but larger increase occurs after 16 minutes (point "B").

Following the loss of the vacuum at "C", there was no applied pressure gradient across the laminate and so all sensors recorded the applied pressure until the end of the test. As a result, this panel (Laminate B) experienced no resin bleeding, and no compaction. There was no resin pressure gradient through the laminate thickness after 23 minutes (recall Figure 4-8), therefore no flow occurs.

	Elapsed Time (min.)	External Vacuum Gauge Reading	Effect on Sensors (Figure 4-9)
A	13	vacuum drops from -12.3 psig to -7.4 psig	• 1/4 point, 3/4 point, and toolplate pressures increase abruptly • mid bleeder pressure starts to increase
B	16	vacuum drops to -4.9 psig	• all sensors jump up by 5-15 psi
C	23	vacuum bag open, all vacuum lost	• all sensors abruptly read the applied pressure

Table 4-1. Sensor reactions to known vacuum losses, shown in Figure 4-9.

The resin pressures registered by the sensors in Laminate Run A, Laminate Run B and Laminate Run C (discussed in the following section) at 105, 115 and 125 minutes after their respective times of pressure application are shown in Figure 4-10. The autoclave pressure at the three times reported varied for Laminate B, resulting in the differences in magnitude of the resin pressure profiles, but the trends are very consistent. This figure illustrates the smaller resin pressure gradient through the thickness of Laminate B, by comparison with Laminates A and C.

The lack of resin flow during Laminate Run B was substantiated in several ways. After the cure cycle, the vacuum bag was opened, and the bleeders separated from the laminate and examined. Only the first of the bleeder layers, placed next to the laminate during cure, had resin in it, and it was not saturated. Also, the final volume fraction of fibres in the laminate was experimentally determined by nitric acid digestion, detailed in Appendix C, to be 0.491. This can be compared to the volume fraction of fibres of the

prepreg, found experimentally to be 0.433 (Appendix D), and the final fibre volume fractions of Laminate A and Laminate C, which are 0.614 and 0.596 respectively (Appendix C). Clearly very little resin has been lost from the laminate.

4.4. Laminate Run C

Due to the difficulties of processing very thick laminates, the next laminate was a repeat of the first laminate run, Laminate Run A. Thus the laminate was a $(0/90_2/0)_{12}$ and the cure cycle was the same as that for Laminate Run A, as shown in Figure 4-11.

In addition to the interface, 1/4 point, 1/2 point, 3/4 point, and toolplate sensors, as described for Laminate Run A, three sensors were placed in the bleeder layers:

- between the 12th and 13th bleeder plies (lower bleeder)
- between the 24th and 25th bleeder plies (mid bleeder), and
- between the 42nd and 43rd bleeder plies (upper bleeder).

The thirty-six bleeder layers of Laminate Run A were increased to forty-eight for this test with the intention that the resin flow would not reach the upper bleeder sensor, as explained for Laminate Run B. However, during the filling and bagging process, the lower and mid bleeder sensor assemblies became damaged, and so could not be used.

Figure 4-12 shows the experimental results from Laminate Run C, while the first one hundred minutes are enlarged in Figure 4-13.

The results from Laminate Run C are similar to those of Laminate Run A (recall Figure 4-4), but not as consistent. As before, all of the sensors show increasing

pressure, after the application of autoclave pressure. In this case however, the interface sensor also reacts almost immediately, although it is very noisy, as does the upper bleeder sensor. It is thought that the interface and upper bleeder sensors read pressures higher than the vacuum registered by the external vacuum gauge due to a small leak in the vacuum bag. If this leak were at a position removed from the vacuum line, a pressure difference could exist horizontally across the laminate, resulting in the conflicting readings.

One explanation for the slow response of the toolplate and 1/2 point sensors in this laminate is that if the fibres around the tip of a sensor tube do not come together tightly there will be a gap that is initially not filled with resin. This could occur due to too large of a misalignment of the tube with the fibre axes. In such a case, the sensor will register the pressure in the gap, and not in the resin.

In Laminate Run C, all the sensors, except the interface, and the upper bleeder sensor, eventually reach the applied pressure. Then at approximately thirty-five minutes, the 1/4 point reading starts to drop, and at approximately fifty minutes, the other laminate sensors start to drop. As in Laminate Run A, the interface sensor shows an increase in pressure corresponding to the decreases registered by the other sensors. Once again, a resin pressure gradient is evident after the sensor responses level off, with the sensors again in the order (with decreasing pressure) toolplate, 3/4 point, 1/2 point, 1/4 point, interface. This is shown in Figure 4-10. The pressure profiles for Laminate A and Laminate C differ only in the magnitude of the pressures reported.

The results from Laminate Run C are very similar to those from Laminate Run A. The differences between the two tests can be attributed to a slight loss of vacuum across the vacuum bag, as described earlier. Both the interface and upper bleeder sensors

read increasing pressures with the pressurization of the autoclave, and the upper bleeder sensor shows an elevated pressure for the duration of the test. Inspection of the bleeder layers after the test showed that a very small amount of resin had been absorbed up the centre of the bleeder stack to the level of the upper bleeder tube. There was not, however, enough resin present in the area to surround the end of the tube so that the sensor could read a resin pressure. Overall, there was less flow and less of a drop in the resin pressure throughout Laminate Run C, compared to Laminate Run A. Less of a vacuum results in less of a pressure gradient across the laminate, which translates to less driving force for resin flow. Evidence of this decreased flow is the lower resin mass loss and the lower final volume fraction of fibres of this laminate, compared to Laminate A, as will be seen in Sections 5.1.2. and 5.1.3. respectively.

4.5. Post-Gelation Behaviour

At the end of each laminate run the resin is solid. Thus the resin pressure is no longer transmitted from fluid resin to sensor fluid, as occurred before the resin gelled. The applied pressure was reduced in steps, and in Laminate Run A raised briefly to 50 psig (446 000 Pa) and released, in order to investigate the response of the sensors. This response was then examined to determine what the sensors measure after gelation of the resin occurs.

In Laminate Run A, the 1/4 point sensor did not step down with the other sensors consistently (Figure 4-4), and it appeared to react to the autoclave temperature, decreasing with decreasing temperature. Examination of the tube for this sensor revealed that it had become sealed, no doubt by the migration of catalysed resin (or catalyst) up the tube. Since the tube was sealed, no pressure change was felt by the diaphragm. None of the other tubes in this laminate were found to be sealed.

In Laminate Run C (Figure 4-12), the toolplate, 1/4 point, and 1/2 point sensors react similarly to the temperature drop at the end of the cure cycle, and respond erratically to the pressure drops. It was found, after the test, that the toolplate and 1/4 point sensors were also at least partially sealed with cured resin. The 1/2 point sensor tube was likely partially blocked also, however, this could not be verified.

When a tube is sealed with cured resin, the sensor assembly becomes a fixed volume system. The pressure in the laminate is no longer transmitted to the sensor, but the temperature is. As the temperature drops, the liquid resin in the tube shrinks, thereby releasing some of the pressure against the sensor diaphragm. A drop in sensor resistance after a tube assembly has become blocked indicates a drop in temperature, not a drop in pressure.

The majority of the sensors in all the laminates respond to the stepping down of the applied pressure at the end of the cure cycle. (See Figures 4-4 and 4-12.) The laminates are now solid and cannot transmit pressure directly to the sensor assemblies. However, the tubes are still filled with fluid and so, for each sensor tube, there must be a boundary between these two media. Consider one such boundary. It is formed when the resin becomes solid, at which time the full pressure is applied to the laminate. The spacing of the crosslinked network of the solid epoxy matrix is determined by the resin pressure at the time of gelation. Resin which gelled at a lower pressure will have a larger network spacing than resin which gelled at a higher pressure.

As the autoclave pressure is reduced, the laminate expands elastically, increasing the network spacing and pulling the boundary slightly away from the tube, thereby releasing some of the pressure on the sensor diaphragm. For a given autoclave pressure drop, the pressure change throughout the laminate will vary, because of the resin pressure

gradient across the laminate thickness. Resin which gelled at a lower pressure will expand less, because it experiences a smaller pressure change.

As the autoclave pressure gets close to atmospheric, the sensor responses become similar. At the end of Laminate Run A the (unsealed) sensors all correctly register the applied pressure throughout the short pressure spike. The network spacing throughout the laminate has become constant, because the whole laminate is now at a constant pressure.

4.6. Figures

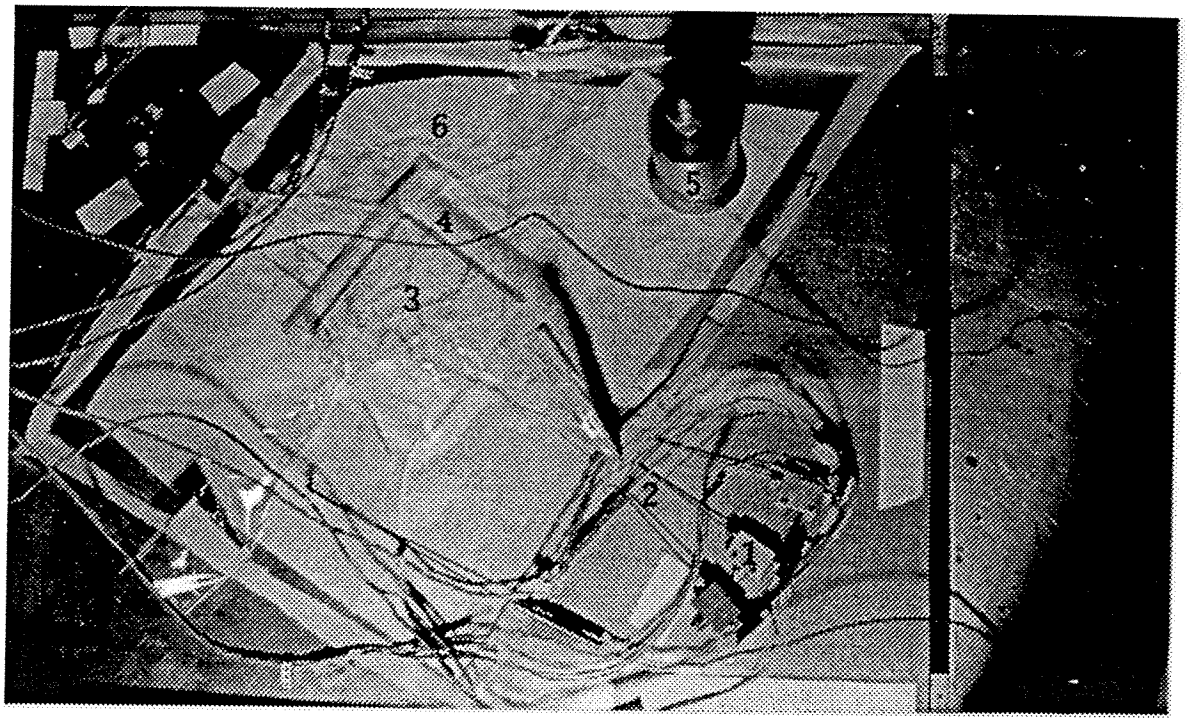

Figure 4-1. Laminate Run A vacuum bag assembly.

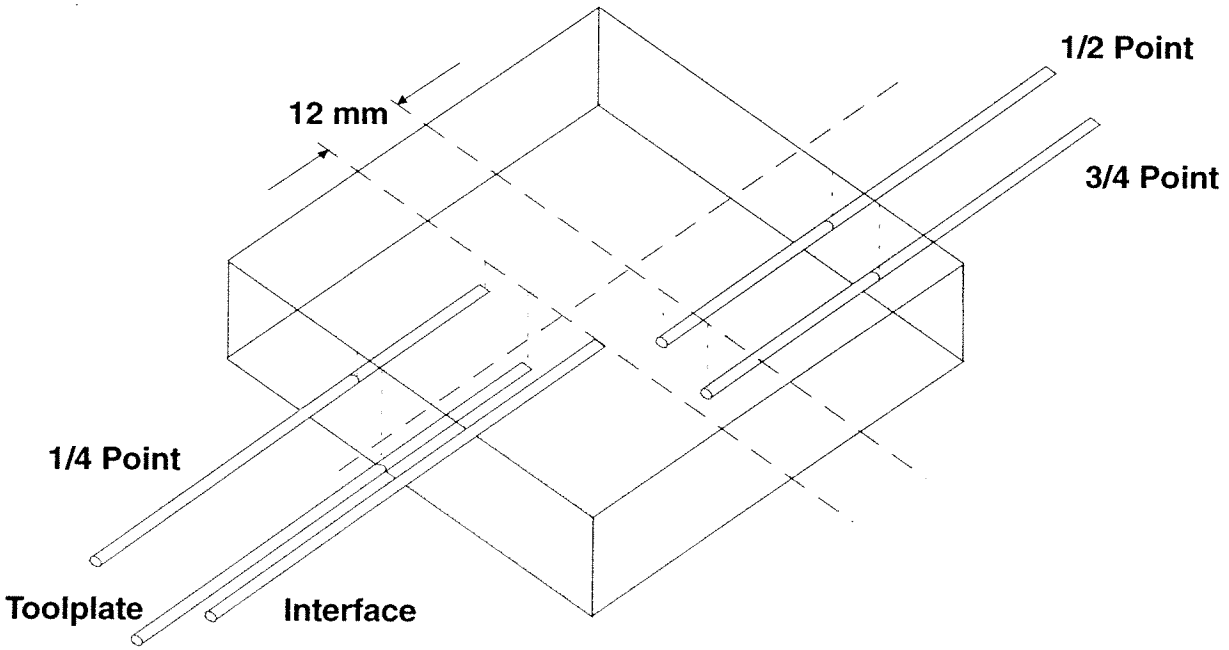

Figure 4-2. Placement of sensor tubes in Laminate Run A.

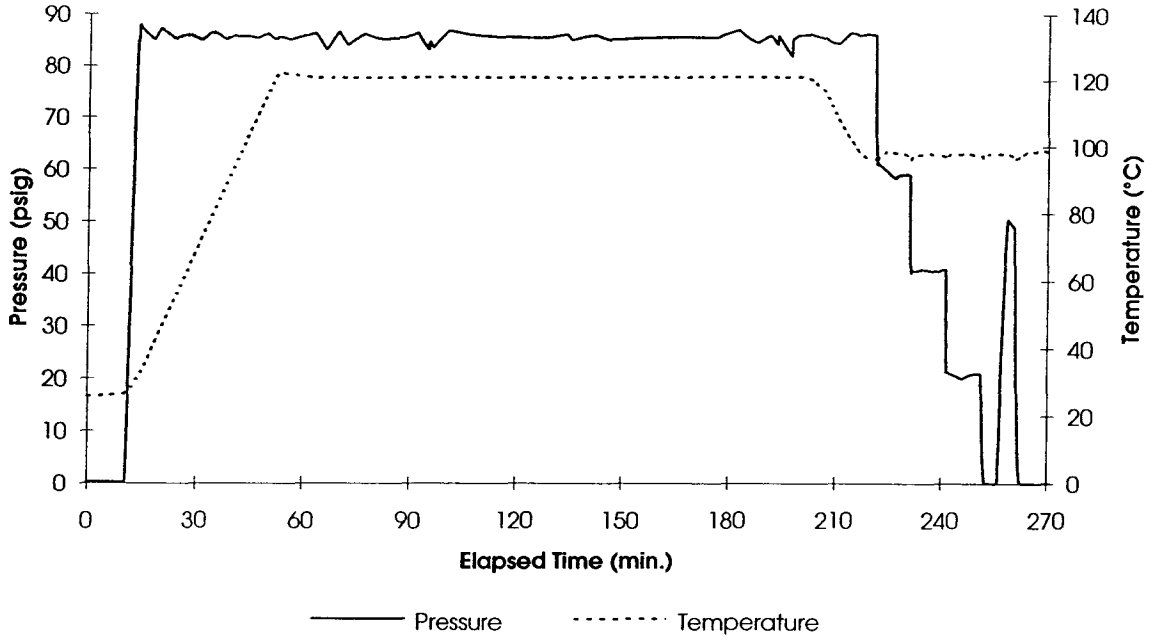

Figure 4-3. Cure cycle for Laminate Run A.

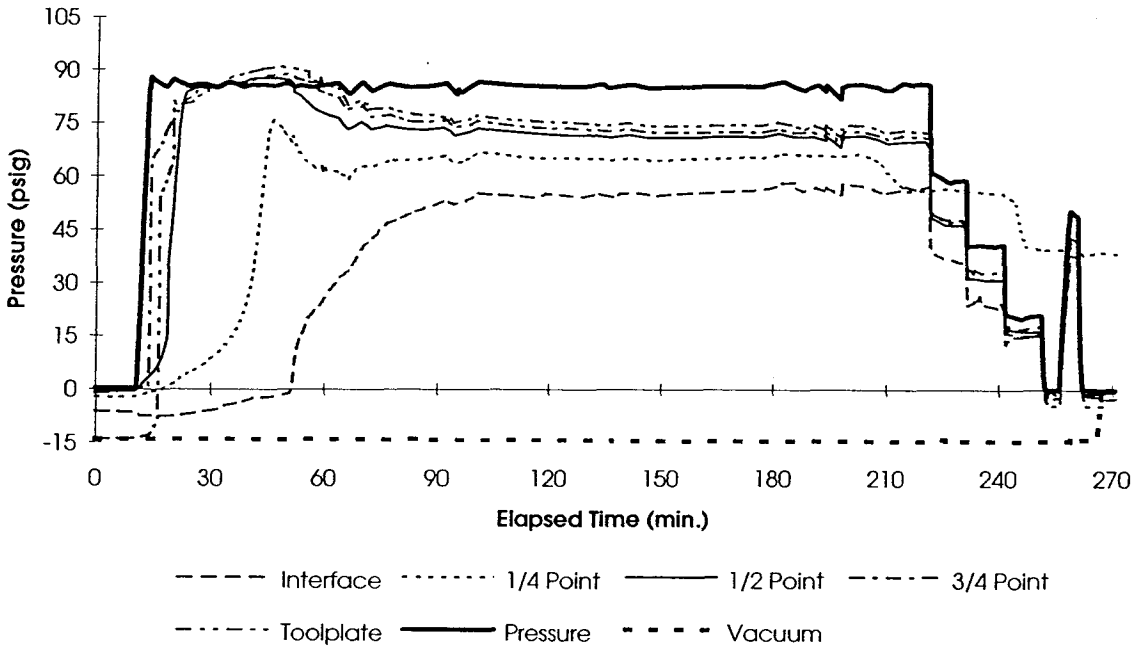

Figure 4-4. Resin pressure throughout the cure cycle for Laminate Run A.

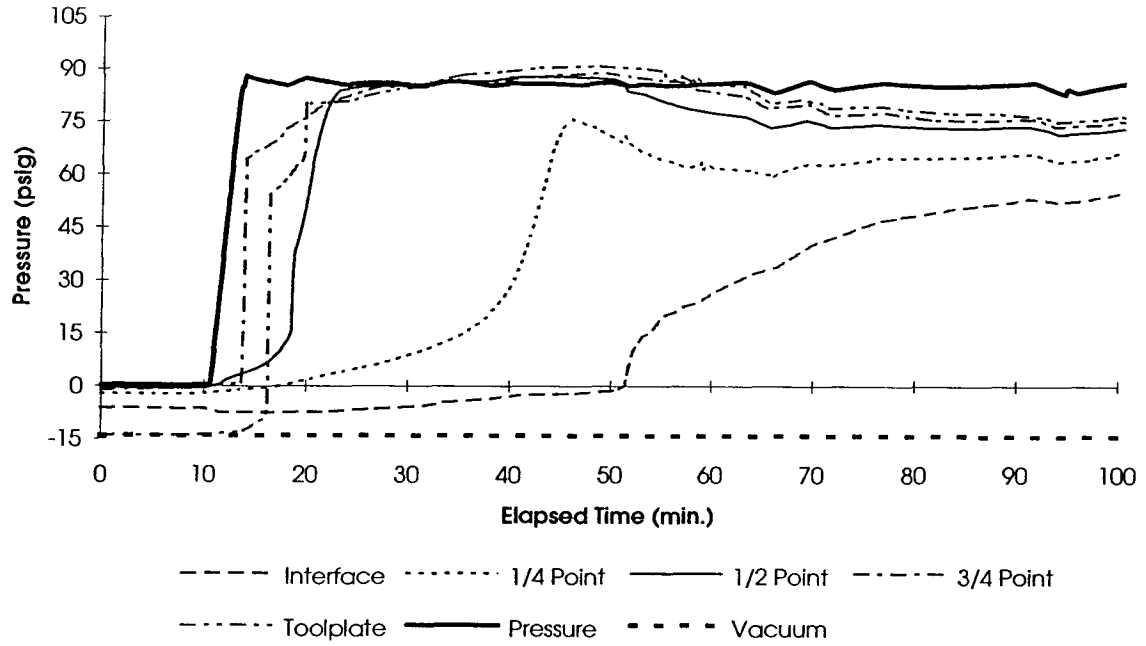

Figure 4-5. Resin pressure over the first 100 min. of cure cycle for Laminate Run A.

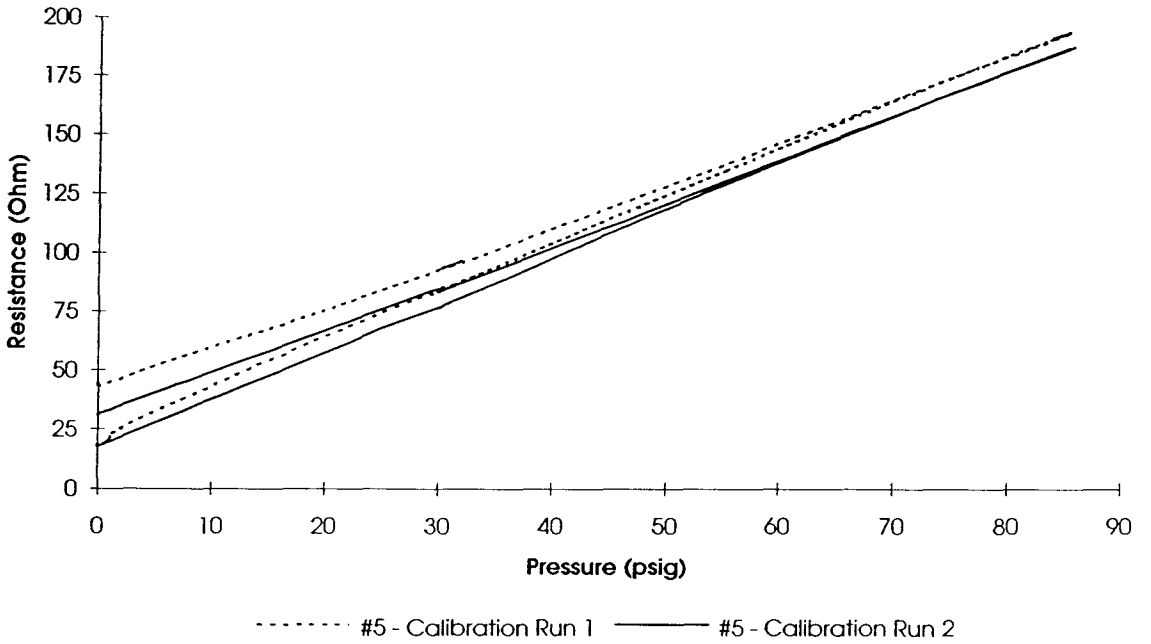

Figure 4-6. Two calibration curves for Sensor #5.

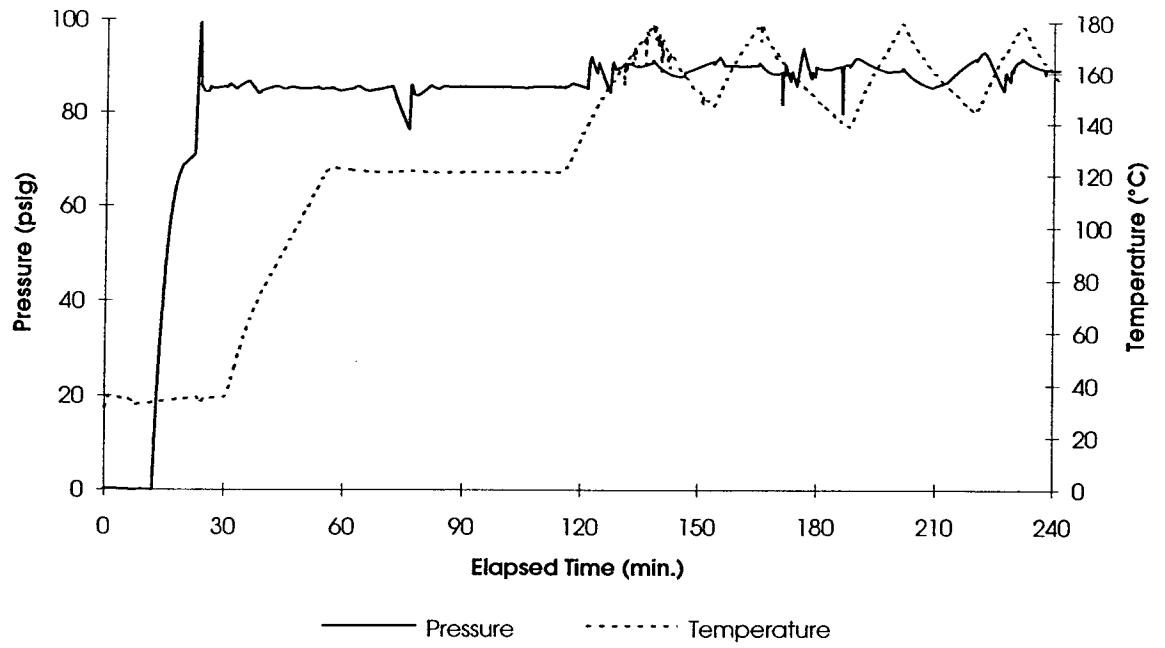

Figure 4-7. Cure cycle for Laminate Run B.

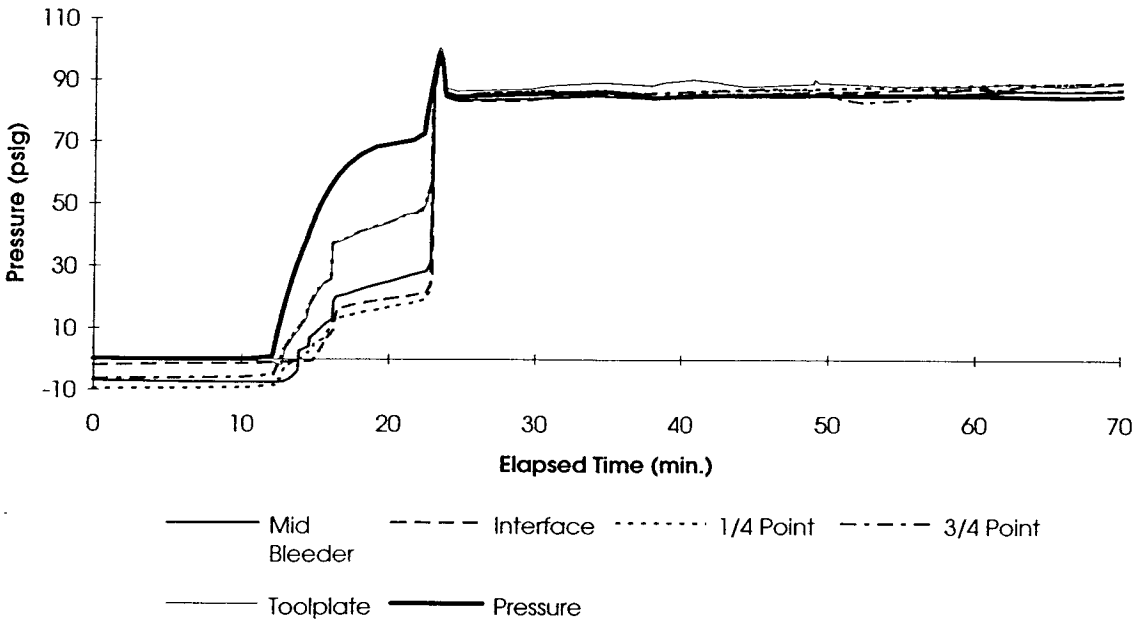

Figure 4-8. Resin pressure over the first 70 min. of cure cycle for Laminate Run B.

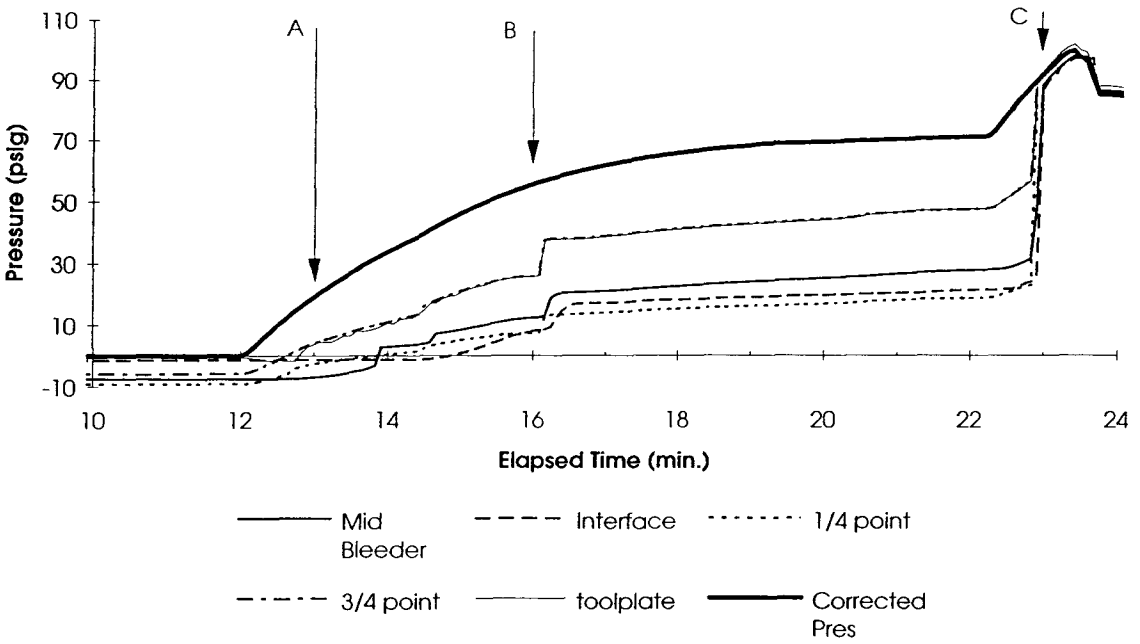

Figure 4-9. Resin pressure over the first 24 min. of cure cycle for Laminate Run B.

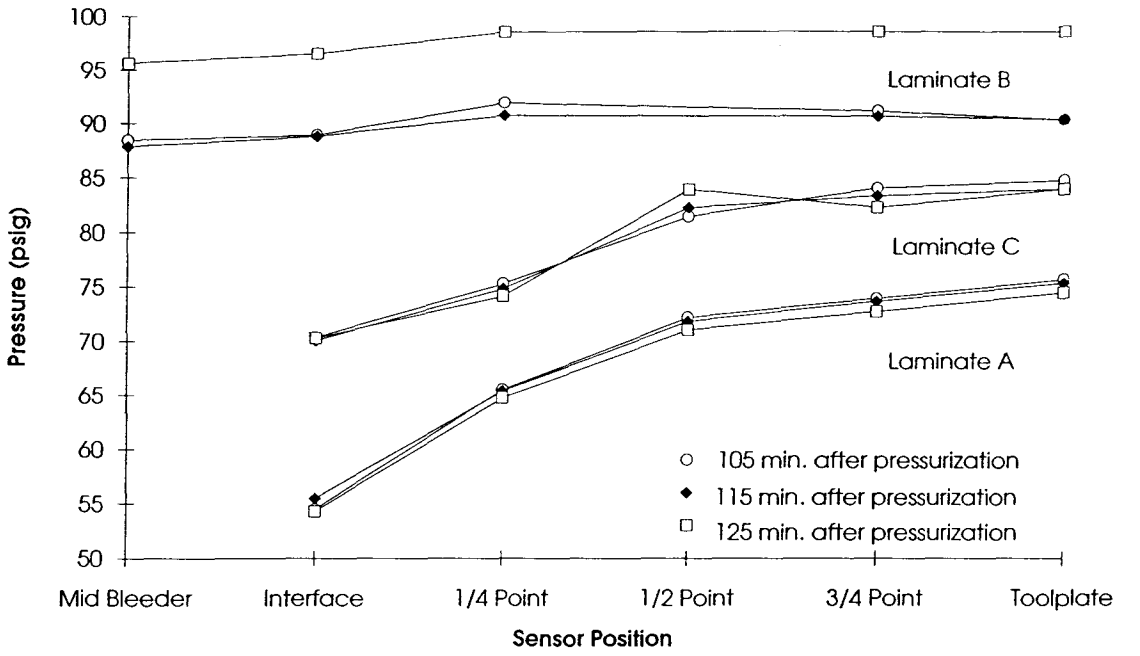

Figure 4-10. Resin pressures at 105, 115, and 125 min. after pressure application for Laminate Runs A, B and C.

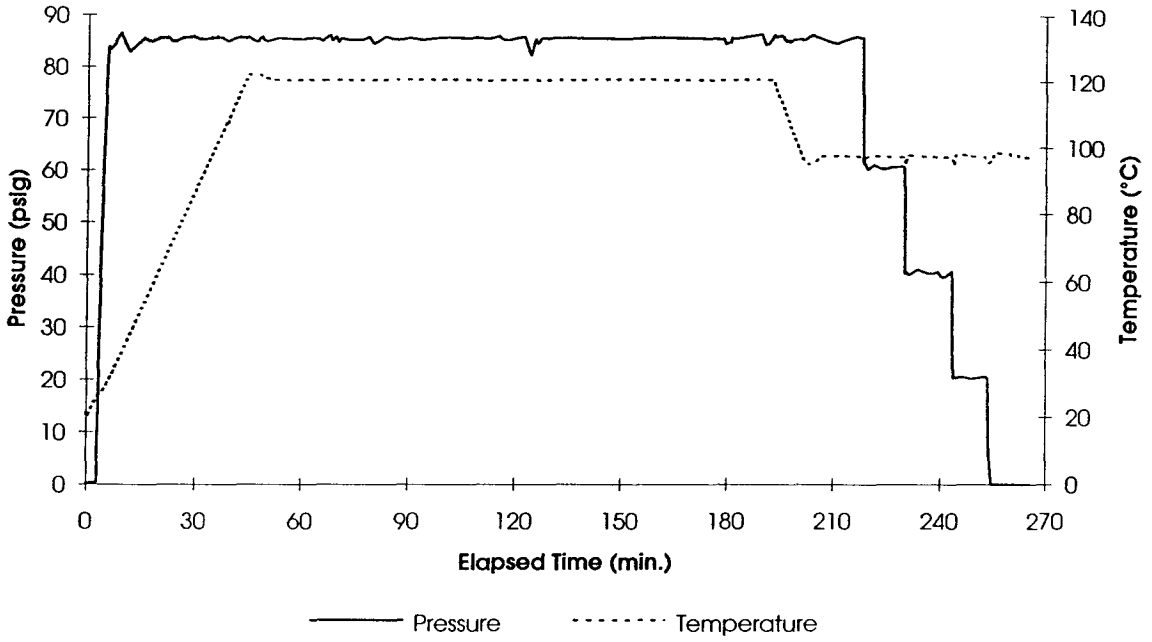

Figure 4-11. Cure cycle for Laminate Run C.

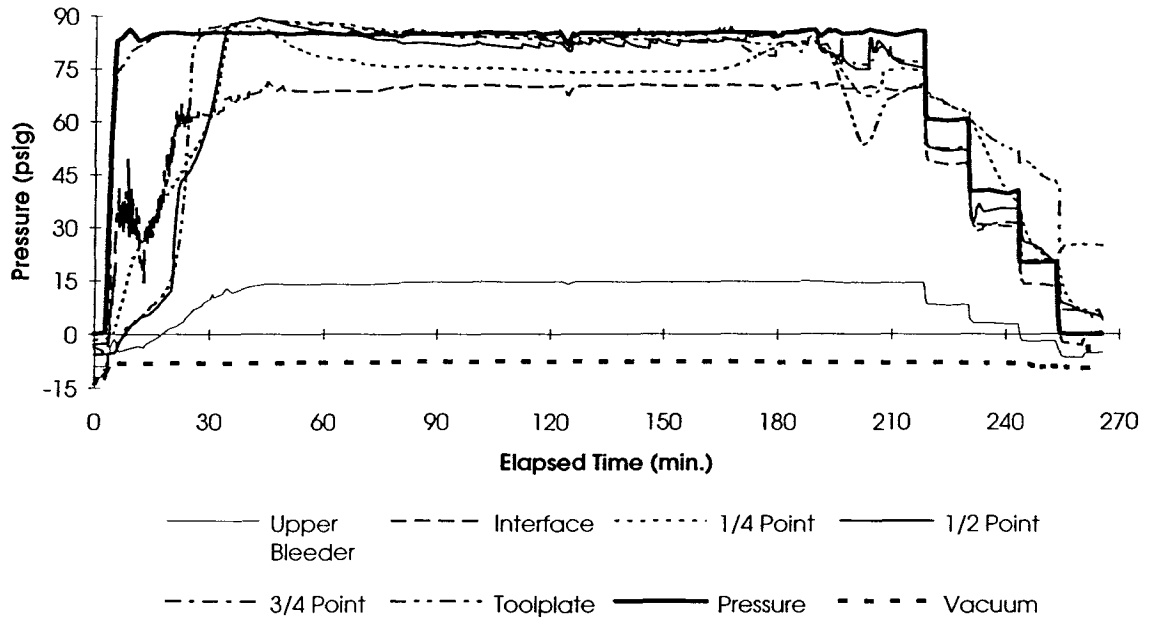

Figure 4-12. Resin pressure throughout the cure cycle for Laminate Run C.

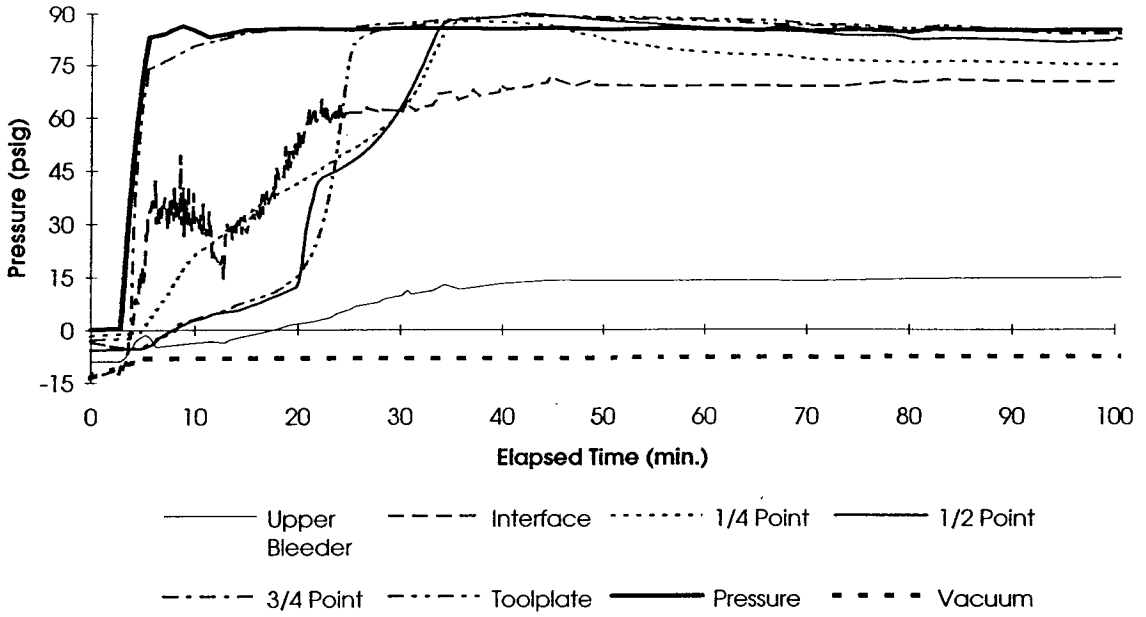

Figure 4-13. Resin pressure over the first 100 min. of cure cycle for Laminate Run C.

Chapter 5: Comparison With Model Results

In Chapter 4, the sensor responses were explained from a physical perspective. In this chapter, the experimental results of the bleed systems, Laminate Run A and Laminate Run C, will be compared to simulation results based on a mathematical model developed for the autoclave vacuum degassing process.

A computer simulation, LamCure [10], described in the literature review, was used to predict the properties of the laminate throughout the cure cycle for various initial conditions. This simulation includes the heat transfer and resin flow models of Loos and Springer [3] and the resin flow model of Davé et al. [15, 17]. Recall that the experimental resin pressure profiles show a pressure gradient extending through the entire laminate thickness from the start of a test (Figure 4-4). This agrees best with the Squeezed Sponge Model of References [15,17] rather than the Sequential Compaction Model of Reference [3]. Therefore the former resin flow model has been used in the comparisons of this chapter. As described in Chapter 2, the Squeezed Sponge model is based on the soil mechanics theory of flow through consolidating porous media. The amount of load supported by the fibre bed for a given ratio of resin to fibres is determined from experimental results reported by Gutowski [18]. Once the fibre bed pressure is determined, the resin pressure throughout the laminate thickness is calculated from a force balance on each lamina and the resin velocity is determined from D'Arcy's Law (Equation 2.1). The input file used for this simulation is shown in Appendix E.

The resin pressure distribution predicted by LamCure for a flat, 10 cm by 10 cm, 48 ply, AS4/3501-6 carbon fibre reinforced epoxy laminate with the same cure cycle as applied

to Laminate Run A is shown in Figure 5-1. The first curve, labelled "Top Ply" is the resin pressure predicted in the centre of the top ply of the laminate. The following curves (1/4 Point, 1/2 Point, etc.) are the resin pressures at the same points in the laminate as the sensors were inserted, as indicated. "Pressure" and "Vacuum" are the applied conditions, and the "Resin Height" curve indicates on the right-hand vertical axis the amount of resin that has flowed into the bleeder layers.

The resin pressure throughout the laminate in Figure 5-1 drops to zero within 30 minutes of the application of external pressure. This did not occur with the experimental results, shown in Figures 4-4 and 4-12. However there are several properties that can change this distribution, the most likely being the initial degree of cure of the resin in the prepreg. Prepreg ages, albeit slowly, from the moment of production, through the cooling and storage stages, and the thawing and lay up of the prepreg into the laminate [22]. In addition, the particular prepreg used in the experiments described here, was stored for much longer than the manufacturers recommended shelf life of 12 months (at -18°C). The importance of the initial degree of cure of the resin is further explained in the following section.

A property of the laminate fibre bed which is also very important is the permeability normal to the fibre axes. Some experimental work has been done to determine this permeability, but no clear value has been found [14]. It is possible that there is a large batch-to-batch variation in permeability even within one material system. Decreasing the permeability of the laminate was found to have essentially the same effect on the resin pressure distribution predicted by LamCure as increasing the initial degree of cure of the resin. It was decided therefore to limit the simulation comparisons to changing the initial degree of cure of the resin.

5.1. Determination of the Apparent Initial Degree of Cure of the Resin

During the layup of the final laminate (Laminate C) the prepreg felt less tacky than was expected which led to speculation that a significant degree of cure had already been reached in the prepreg before the initiation of the cure cycle.

The initial degree of cure of the resin, α_i, in a composite laminate affects the amount of resin flow which occurs during the cure cycle. As the degree of cure of the resin increases the viscosity of the resin increases and therefore less flow occurs for a given pressure gradient. For example, consider two laminates, identical except for α_i, and subject to the same cure cycle. In the laminate with the higher initial degree of cure, resin flow will occur more slowly, and gelation (solidification of the resin) may occur while a pressure gradient remains through the laminate thickness. In terms of resin pressure, the laminate with the higher initial degree of cure will require longer for the pressure to drop throughout the laminate, due to the reduced resin flow. If the resin gels before the pressure drop is complete, then a resin pressure gradient will exist in the laminate at gelation.

The results of Reference [10], for their laminate designated #3, can be directly compared to Laminate Run A, as each had essentially the same cure cycle, layup and material. This laminate was made with prepreg from the same roll as Laminate Runs A-C reported here, but ten months earlier.

Reference [10] reported that the pressure in the laminate increased with the applied pressure, then within five minutes of pressurization, all of the sensors showed decreasing pressure, without any apparent order through the laminate thickness. The

pressure throughout dropped completely by 40 minutes after the application of pressure.

In Laminate Run A, the pressure registered by all sensors, except that at the interface, increases with the autoclave pressure, and is only starting to drop at 40 minutes after the application of pressure.

Thus the resin flow reported in Reference [10] laminate appears to occur earlier, and more completely than that in Laminate Run A. These results resemble the simulation results for an initial degree of cure close to zero. Variation in initial degree of cure of the resin in the prepreg reasonably accounts for the differences in the results from these similar laminates indicating that the prepreg used in Laminates A - C had an advanced α_i.

The fully cured resin mass fraction of the remaining prepreg was experimentally determined by acetone digestion in order to get an indication of the initial degree of cure of the experimental laminates. A description of the method used is given in Appendix F. The values determined from three samples ranged from 0.11 to 0.16, producing an average value of 0.13. Thus 13% of the resin mass in the prepreg was already fully cured before the initiation of the cure cycle. The initial degree of cure of the resin, α_i, is a measure of both full and partial cure of the resin, therefore α_i of the prepreg used here must be higher than 0.13. The three laminate runs described in this work took place within a four month period, with the prepreg stored in a freezer when not in use, so the degree of cure of the prepreg will not have advanced significantly within this time.

The LamCure simulation was run several times for the same system, but with α_i values of 0, 0.15, 0.25, 0.35, 0.40 and 0.45. In the following sections, the simulation results are compared with the sensor responses and experimental results from the actual laminates.

5.1.1. Resin Pressure

The importance of the initial degree of cure on the resin pressure distribution in the laminate can be seen by comparing Figures 5-1 to 5-6. These figures show the predicted resin pressures for α_i = 0, 0.15, 0.25, 0.35, 0.40 and 0.45. Increasing the initial degree of cure of the resin significantly affects the resin pressure distribution through the laminate thickness during cure.

Prior to the application of pressure, the vacuum drawn on the laminate reduces the pressure in the centre of the top ply, next to the bleeder. This effect is of the order of 10 psi (69 000 Pa) for α_i = 0, and decreases with increasing initial degree of cure until for α_i = 0.45 it can just barely be seen.

When the external pressure is applied, the top ply resin pressure increases, but starts to drop off as flow occurs, before the total applied pressure is reached. The discrepancy between the applied pressure and the highest pressure reached in the top ply decreases with increasing initial degree of cure of the resin until, at α_i = 0.45, the full applied pressure is felt in the top ply. This pressure difference is proportional to, but not the same as the initial pressure drop due to the vacuum.

The curves documenting the resin height in the bleeder verify that drops in resin pressure are due to flow of the resin into the bleeder. For α_i = 0, the resin height in the

bleeder slowly increases from the beginning of the test, then increases at a noticeably higher rate with the application of pressure. As the initial degree of cure increases, the resin height in the bleeder at any particular time decreases. For α_i = 0.45, no resin enters the bleeder until the autoclave pressure is applied, and the amount of resin in the bleeder then increases much more gradually than for the case of α_i = 0. Thus in this case, resin flow occurs only after the autoclave pressure is increased, and the flow is slower than that which occurs when α_i = 0.

The resin pressure at the 1/4 point of the laminate (between the 12th and 13th laminae) starts to decrease approximately 8 minutes after the top ply pressure for α_i = 0, and it drops to a stable pressure of about 0 psia (0 Pa). As the initial degree of cure of the prepreg increases, the time before the pressure drop in the 1/4 point increases, and the sharpness of the drop decreases. For example, when α_i = 0.15, the 1/4 point pressure starts to drop off 13 minutes after the top ply pressure drops. For α_i = 0.35, the 1/4 point pressure starts to drop after 26 minutes and the stable value of the resin pressure is about 37.5 psia (259 000 Pa). For α_i = 0.45, these values are 33 minutes and 66 psia (455 000 Pa) respectively.

Similarly, when α_i = 0 the 1/2 point pressure starts to decrease about 6 minutes after the 1/4 point, with the 3/4 point and toolplate pressures starting to decrease essentially together 6 minutes later. In this case, the resin pressure drops to zero throughout the entire laminate. Again comparing these results with those for prepreg with a higher initial degree of cure, slower responses and smaller pressure drops are seen. For initial degrees of cure greater than 0.25, the resin pressure throughout the laminate never drops to zero. For example, in the case of α_i = 0.35, the top ply pressure is about 2.5 psia (17 000 Pa), the 1/4 point pressure stabilizes at about 37.5 psia (259 000 Pa), the 1/2 point at about 64.5 psia (445 000 Pa), and the 3/4 point and toolplate at 83 psia

(570 000 Pa) and 90.5 psia (624 000 Pa) respectively. For α_i = 0.45, practically no pressure drop can be seen for the 3/4 point or toolplate position, and the drop in the 1/2 point is quite small (about 6.5 psi (45 000 Pa) from the applied pressure).

Comparing the results from Laminate Run A and Laminate Run C (Figures 4-4 and 4-12) with the simulation predictions with an initial degree of cure of 0.15, one can see that agreement is slightly better than for the 0 initial degree of cure case. Comparing these results to the initial degree of cure of 0.35 or 0.40 cases shows much better agreement. The shapes and distribution of the curves match, with the 1/4 point sensors dropping off first at about 30 minutes after pressurization, then the 1/2 point sensors about 10 minutes later, and with the 1/2 point sensor stabilizing at a slightly lower pressure than the 3/4 point and toolplate sensors. Table 5-1 summarizes these results.

	time* of 1/4 point drop (min.)	stable 1/4 point pressure (psia)	time* of 1/2 point drop (min.)	stable 1/2 point pressure (psia)
0	11	0	17	0
0.15	16	0	26	0
0.25	21	0	30	0
0.35	29	37.5	37	64.5
0.40	32	50.5	41	83.5
0.45	36	64	47	94
Laminate A	36	80	41	86
Laminate C	35	89	43	96-98

* for the purpose of this comparison, time is measured from the start of autoclave pressurization

Table 5-1. Magnitude and timing of resin pressure drops in simulated and real laminates.

The stable pressures for the 1/4 point and 1/2 point of Laminate A and Laminate C are high compared to the simulation results. However the timing of the pressure drops, and the distribution of resin pressure through the laminate thickness for the simulations with α_i = 0.35 and 0.40 show reasonable agreement with the experimental results.

5.1.2. Resin Loss

The experimental and simulation results can also be compared with regard to the amount of resin that is lost from the laminate during cure. The final values of resin height in the bleeder for the different initial degree of cure simulations are shown in Table 5-2. It can be seen that a value of α_i > 0.25 can significantly change the amount of resin flow which occurs in the composite laminate during cure.

Initial Degree of Cure of the Resin	Final Resin Height in the Bleeder (m)	Comments
0	0.00436	full compaction
0.15	0.00436	full compaction
0.25	0.00436	full compaction
0.35	0.00353	partial compaction
0.40	0.00260	partial compaction
0.45	0.00193	partial compaction

Table 5-2. Simulation predictions of the amount of resin flow into the bleeder for various prepreg initial degrees of cure.

The simulation results for final resin height in the bleeder presented in Table 5-2 can be changed to resin masses by using the porosity of the bleeder, and the resin density.

These calculations are shown in Appendix G and the results for each initial degree of cure are displayed as mass losses in Table 5-3 below.

The amount of resin lost from Laminate Run A and Laminate Run C was calculated, both from the change in mass per area from the prepreg to the final laminates, and from mass measurements of the bleeder layers before and after the cure cycles. These calculations are shown in Appendix H and the results displayed in Table 5-3, as "laminate" and "bleeder" mass losses respectively.

Mass Loss (g)	Initial Degree of Cure of the Resin					
	0	0.15	0.25	0.35	0.40	0.45
simulation	31.306	31.294	31.276	25.373	18.642	13.830
Laminate Run A laminate	28.738					
bleeder	24.62					
Laminate Run C laminate	20.315					
bleeder	18.92					

Table 5-3. Final resin mass loss values of simulated and real laminates.

Table 5-3 shows that the real laminates produce data which is generally between that of the LamCure predictions with α_i = 0.35 and 0.40.

5.1.3. Laminate Compaction

The compaction of a composite laminate is also affected by the initial degree of cure of the resin in the prepreg. As shown in Figure 5-7, a more fully cured resin has a higher

viscosity for a greater amount of time, thus less resin flow and consequently less compaction can occur in a composite with a higher initial degree of cure before the resin gels. The result is a less consolidated laminate, with a lower volume fraction of fibres. The difference in the compaction of the various laminates is shown in Figure 5-8 which compares the average volume fraction of fibres over the applied cure cycle. Clearly a large difference in laminate compaction behaviour can be caused by a small change of initial degree of cure of the resin. Figure 5-9 further illustrates this by comparing the final volume fraction of fibres of each laminate to the initial degree of cure of the resin matrix.

The final volume fraction of fibres of Laminate A and Laminate C were determined experimentally by nitric acid digestion, as described in Appendix C. These values are displayed in Table 5-4 along with the simulation results which were shown in Figure 5-9.

	Initial Degree of Cure of the Resin					
	0	0.15	0.25	0.35	0.40	0.45
Simulation V_f	0.6868	0.6867	0.6866	0.6376	0.5940	0.5653
Laminate Run A V_f	0.614					
Laminate Run C V_f	0.596					

Table 5-4. Comparison of final average volume fraction of fibres for simulated laminates to results of nitric acid digestion of real laminates.

As found in the previous sections, the experimental values fall between the results of cure simulations with initial degrees of cure of 0.35 and 0.40.

5.1.4. Summary

The simulation predictions have been compared to the experimental results in three different ways. The resin pressure distributions, the mass lost from the laminate during cure, and the final average volume fraction of fibres have all been used to demonstrate the good agreement between experimental results and the simulations with α_i = 0.35 - 0.40. Table 5-5 summarizes these results.

	Laminate A	Laminate C	Simulation α_i = 0.35	Simulation α_i = 0.40
time* of 1/4 point drop (min.)	36	35	29	32
stable 1/4 point pressure (psia)	80	89	37.5	50.5
time* of 1/2 point drop (min.)	41	43	37	41
stable 1/2 point pressure (psia)	86	96-98	64.5	83.5
Mass Loss laminate bleeder	 28.738 24.62	 20.315 18.92	 25.373	 18.642
Final V_f	0.614	0.596	0.6376	0.5940

* for the purpose of this comparison, time is measured from the start of autoclave pressurization

Table 5-5. Summary of experimental and simulation results.

Based on these results, in the following section the responses of the tube sensor assemblies in Laminates A and C will be compared carefully to the simulation predictions with α_i = 0.35 and 0.40.

5.2. Comparison of Experimental Resin Pressure Profiles With Simulation Results for α_i = 0.35 - 0.40.

Careful comparison of the resin pressure profiles for Laminate A (Figure 4-4), Laminate C (Figure 4-12), and the simulations with α_i = 0.35 and 0.40 (Figures 5-4 and 5-5) show that although certain characteristics of the experimental laminates are not predicted by the simulations, the general timing and distribution are well represented. For example, Figure 5-10 shows the resin pressure at the 1/2 point for Laminate A and simulations with α_i = 0.25, 0.35, 0.40 and 0.45.

In the real laminates, there is a lag between the time of pressure application, and the time that the resin pressure increases. After this lag, the resin pressure from the 1/2 point down to the toolplate rises quickly to close to the applied pressure, and then gradually increases before starting to drop off as flow begins. The simulation results do not display these features, rather the resin pressure from the 1/4 point to the toolplate increases with the applied pressure and remains at this pressure until the onset of flow. It is likely that in the real laminates, some consolidation and settling of the laminate occurred as the autoclave pressure increased.

The time at which the resin pressure at each point through the laminate thickness starts to drop is well predicted by the simulations with α_i = 0.35 and 0.40, as is the initial rate of this pressure drop. However the simulations predict lower stable resin pressures for the 1/4 and 1/2 point than occur in Laminate A and C.

At the end of the cure cycle, when the pressure is stepped down, the simulation results are no longer realistic. Once the resin becomes solid the assumptions used for the fluid system are no longer valid.

Overall, the simulation results exhibit good agreement with the experimental results in the region of flow when an initial degree of cure for the prepreg of between 0.35 and 0.40 is used. This is not inconsistent with the experimentally determined cured resin mass fraction of 0.13 which indicates that the initial degree of cure of the prepreg must be considerably greater than 0.13. It must be noted however, that altering other inputs to the simulation, such as the permeability of the fibre bed, could produce results suggesting some other value of α_i. The material parameters used in the simulation come from various sources [10]. Variation in these parameters could be significant from one batch to another, even within the same material system. For example, the permeability used in the simulation, although based on the works of several groups of researchers [10, 15, 17], may not be accurate for the prepreg used in this work.

Further experimentation, with well characterized prepreg is required for absolute verification of the simulation's accuracy. However, this work has shown that the simulation, with α_i= 0.35 - 0.40, produces results which compare well with the measured responses of the tube sensor assemblies, and the experimentally determined characteristics of the laminates.

5.3. Figures

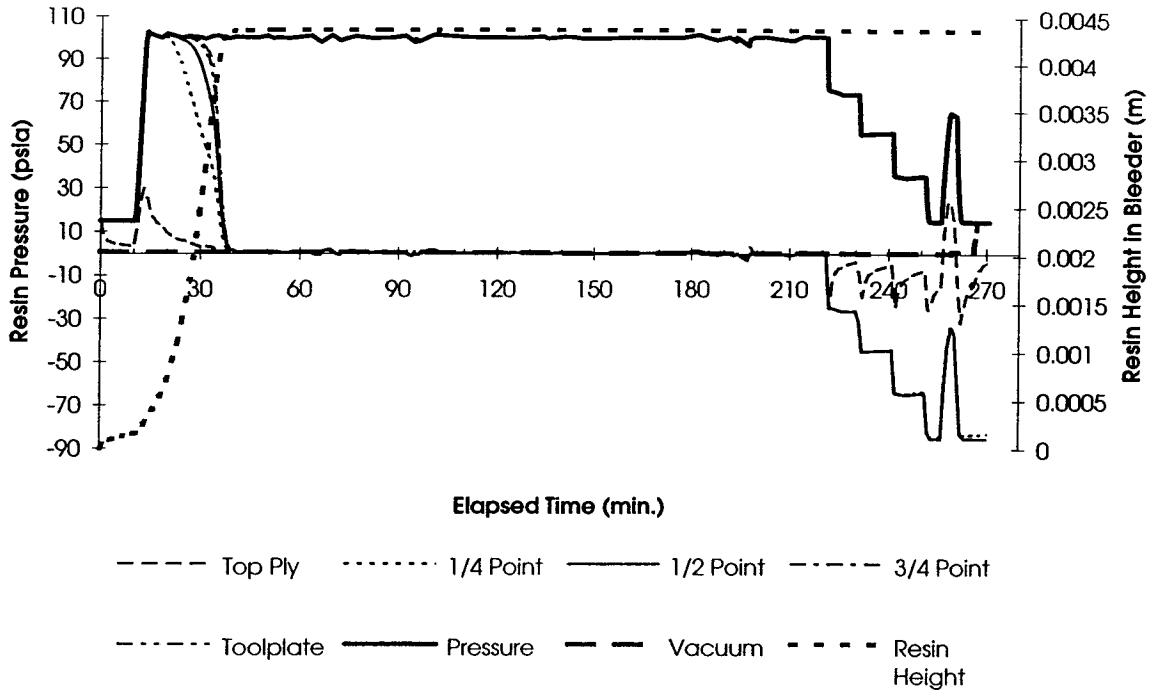

Figure 5-1. Laminate Run A - Simulation prediction for 0 initial degree of cure.

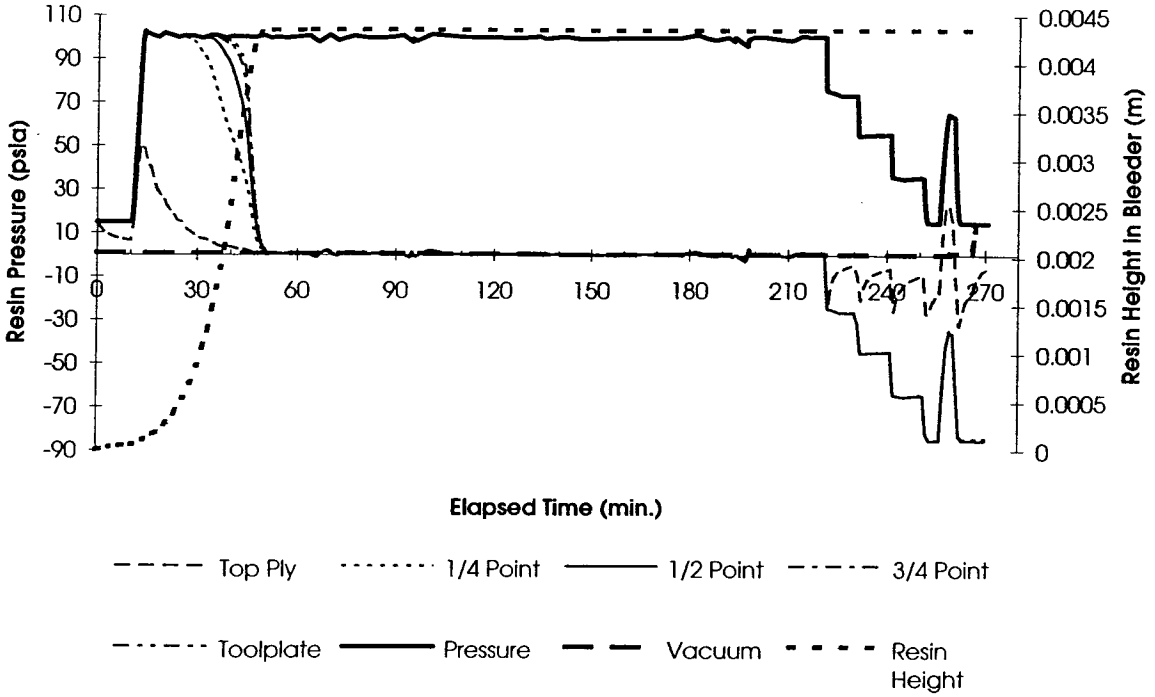

Figure 5-2. Laminate Run A - Simulation prediction for 0.15 initial degree of cure.

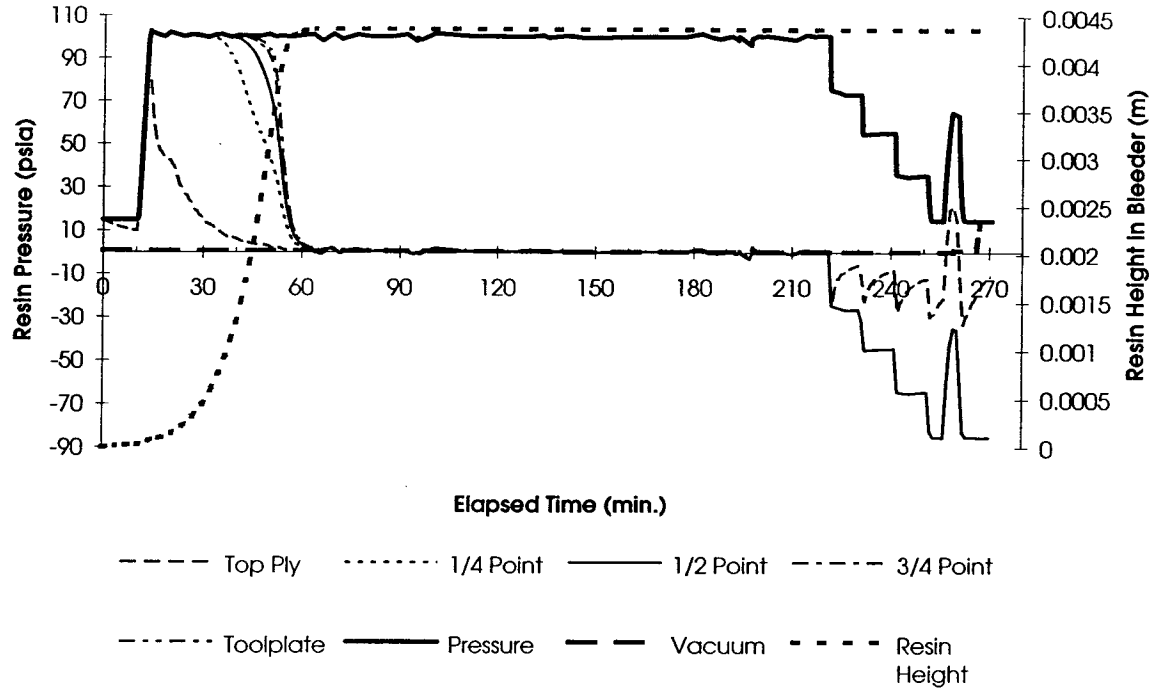

Figure 5-3. Laminate Run A - Simulation prediction for 0.25 initial degree of cure.

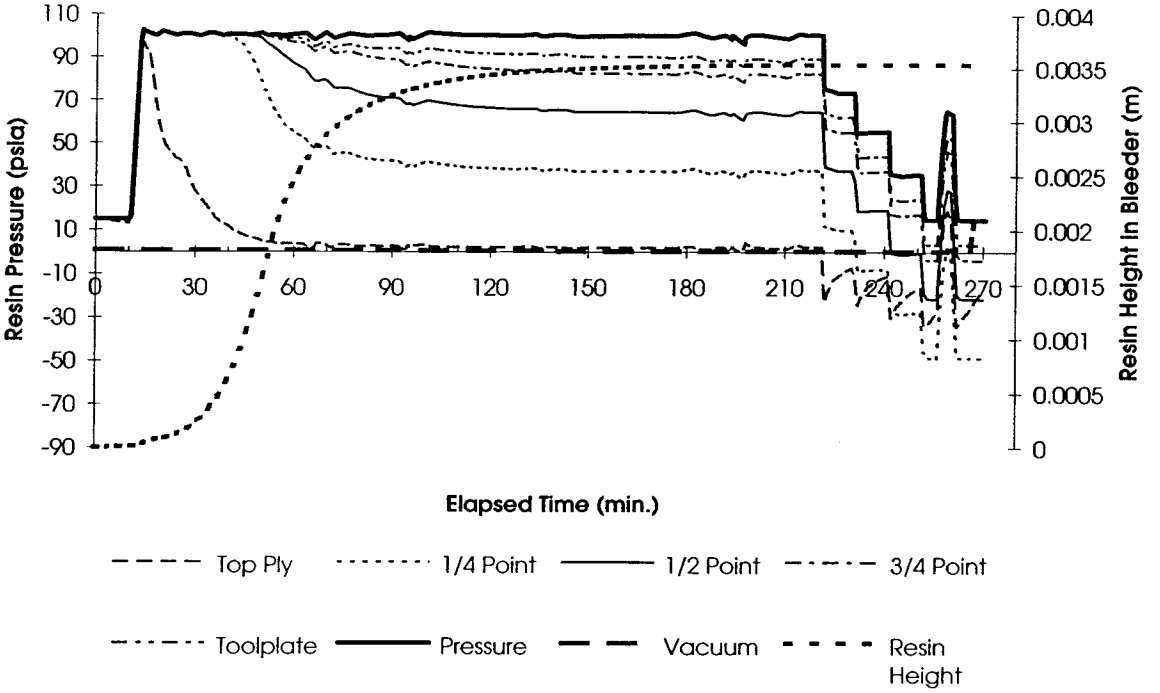

Figure 5-4. Laminate Run A - Simulation prediction for 0.35 initial degree of cure.

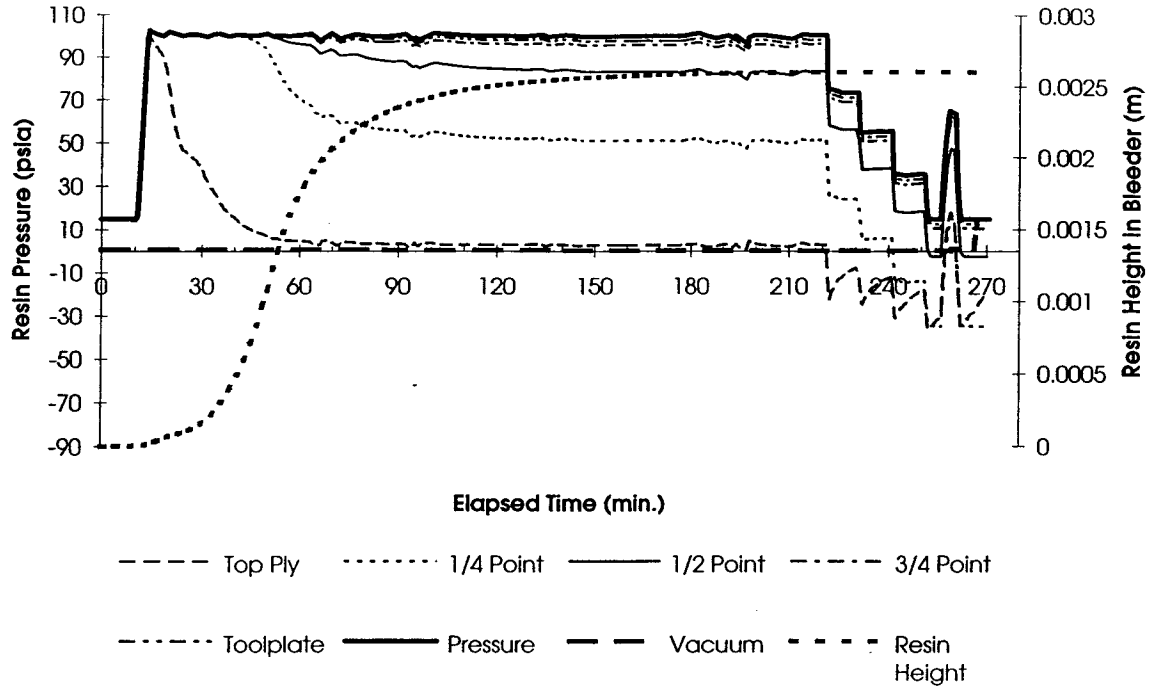

Figure 5-5. Laminate Run A - Simulation prediction for 0.40 initial degree of cure.

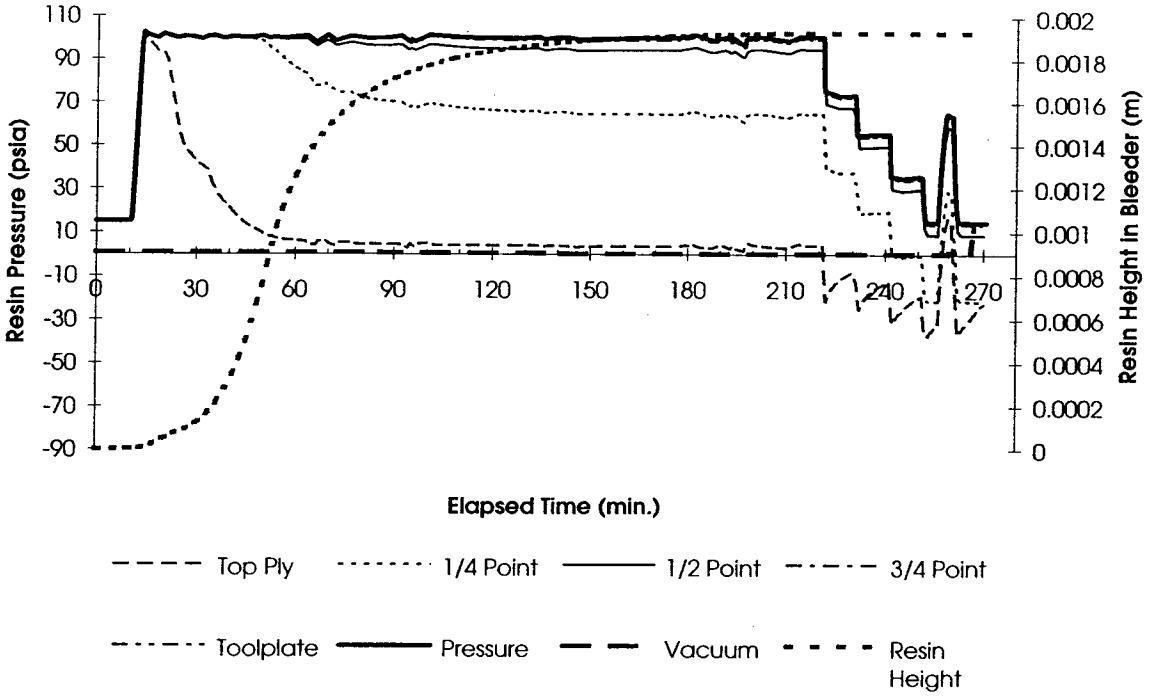

Figure 5-6. Laminate Run A - Simulation prediction for 0.45 initial degree of cure.

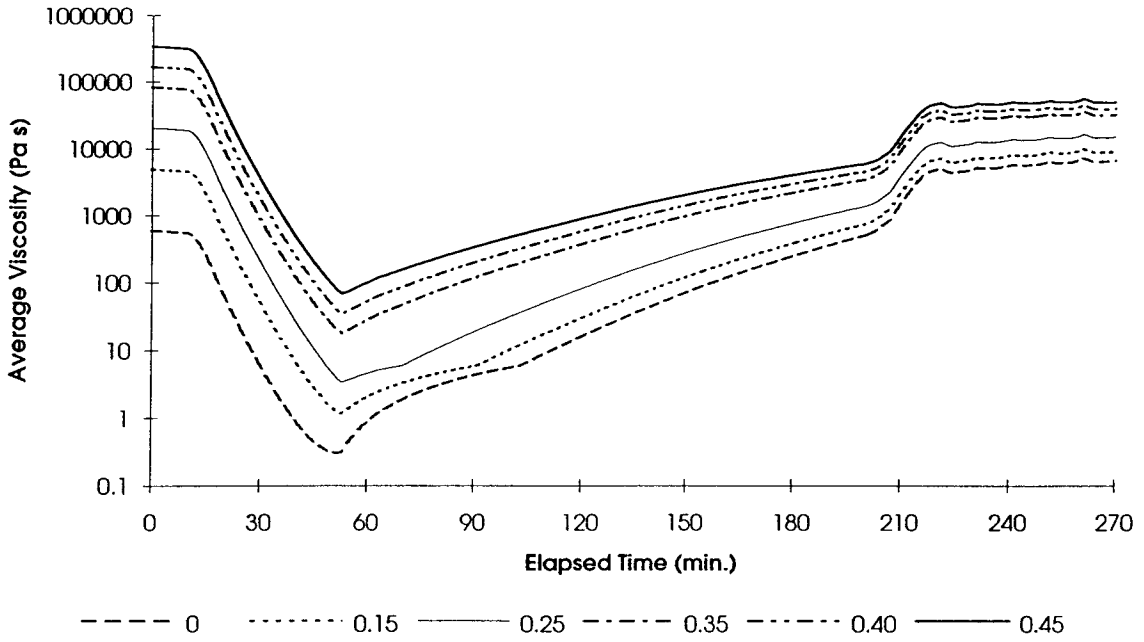

Figure 5-7. Laminate Run A - Simulation predictions of the resin viscosity profile.

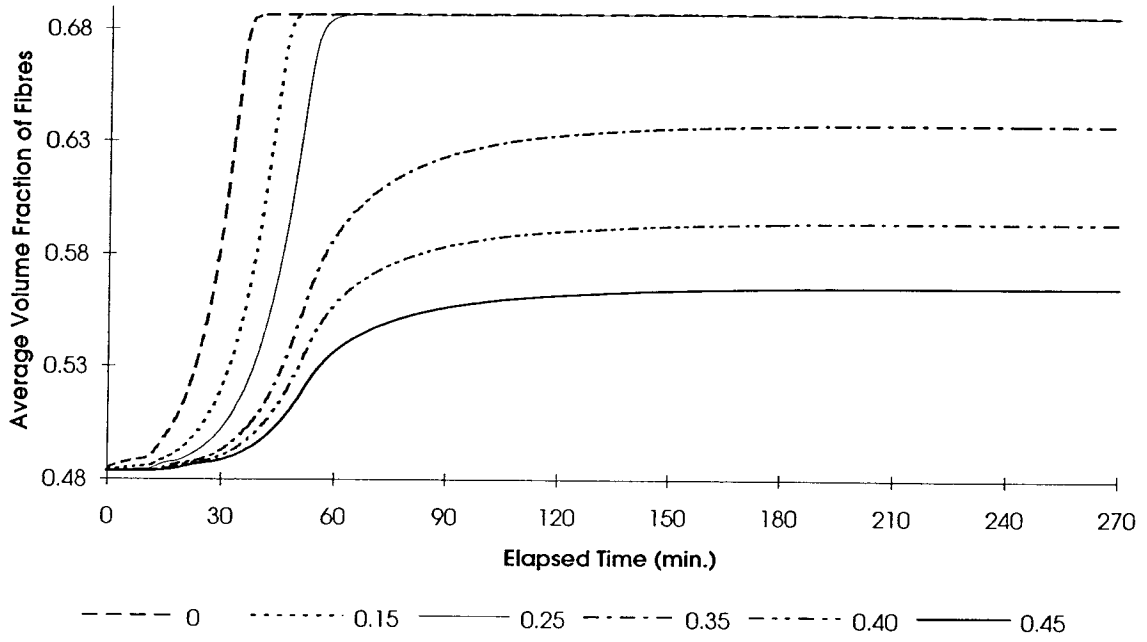

Figure 5-8. Laminate Run A - Simulation predictions of laminate compaction over the cure cycle.

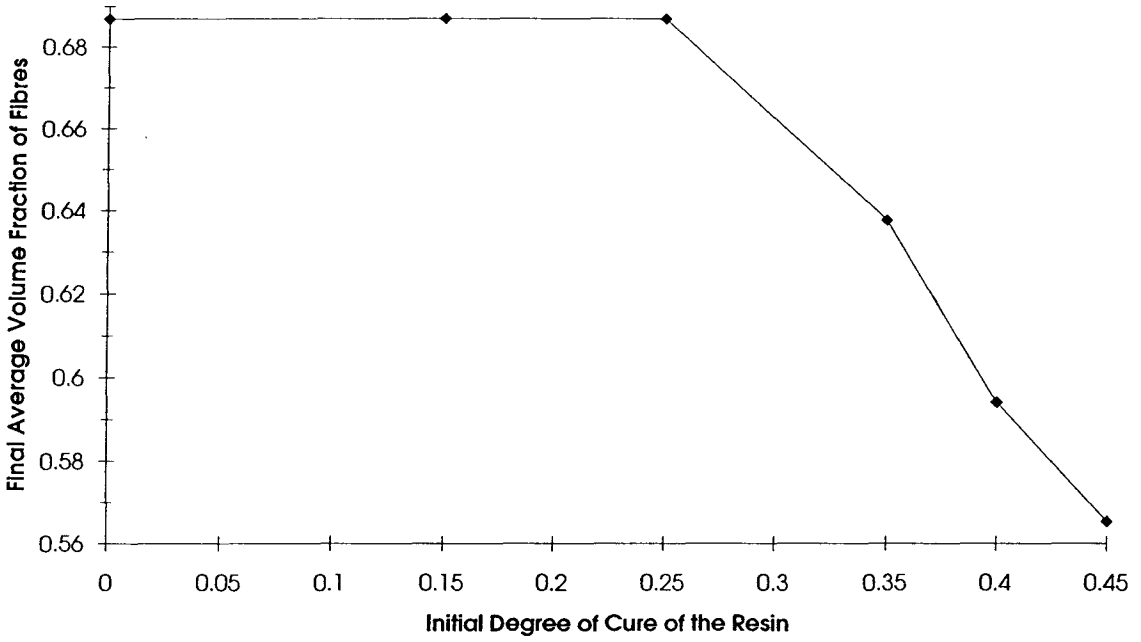

Figure 5-9. Laminate Run A - Simulation predictions of the final volume fraction of fibres.

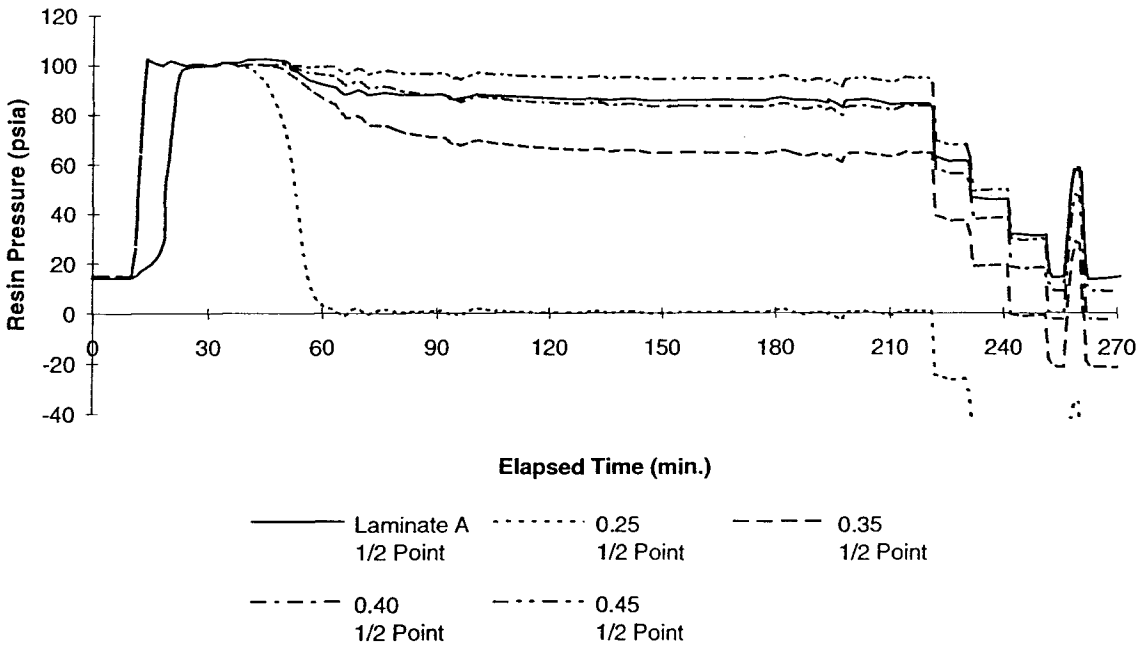

Figure 5-10. Resin pressure at the 1/2 point for simulations and Laminate A.

Chapter 6: Conclusions and Recommendations

6.1. Conclusions

- The tube sensor assemblies are non-hysteritic, absolute devices which produce reproducible, linear results that are stable with time and temperature.

- If a sensor tube becomes sealed, it will no longer measure pressure, but will indicate temperature changes.

- The resin pressure within a laminate increases with the applied pressure until flow begins, at which time the resin pressure drops off progressively through the laminate thickness, from the top surface to the toolplate.

- A resin pressure gradient exists across the entire laminate thickness until full compaction occurs or the applied pressure is released.

- An advanced degree of cure of the prepreg at the start of the cure cycle significantly affects the resin flow and compaction in the laminate during cure.

- The Squeezed Sponge Model [15, 17], as represented in a computer simulation [10] with appropriate material parameters, can produce a reasonable estimation of the resin pressure throughout a laminate during cure.

6.2. Recommendations

The experimental work presented in this thesis shows great promise of furthering the understanding of composite material processing. This method can be used to study laminate resin pressure for the control of voids or the support of honeycomb inserts, or to investigate resin flow and laminate compaction.

Further work is required to verify these results. In addition, because of the complicating factor of initial degree of cure of the prepreg, these tests should be redone with fresh prepreg. For industrial use, the prepreg must be used promptly as the low temperature cure products created as the prepreg ages do not have the same properties as the desired high temperature cure products [23].

In order to understand what is happening in the laminate after gelation, more tests are required to determine what the sensors are measuring after this point in the cure cycle.

Smaller tubing is available. For example, a 33 gauge tube has an outside diameter of approximately 0.2 mm and would fit within a double layer of unidirectional plies. This would reduce even further any disturbance to the resin flow and pressure distribution within the laminate. It is recommended that this smaller tubing be used for further investigation of resin flow in composites. The narrowness and flexibility of the 33 gauge tubes would also enable them to measure the resin pressure in more difficult areas, such as tight corners and honeycomb cores.

Once the pressure distribution in components of various shapes is understood for bleed systems, this technology should be applied to zero bleed systems. Commercially, zero bleed systems are more typical and any further insight into the resin flow and pressure

distribution in these systems would be extremely beneficial to the composites industry. The tube sensor assemblies could also be used as troubleshooting devices to define and pinpoint processing difficulties. Consider, for example, a problem with voids in a certain area of a component. The resin pressure distribution in the problem area throughout the cure cycle could be determined by instrumenting that area with tube sensors. This would show when and where there is a problem, so that remedial action could be taken.

In order for these sensor assemblies to be used in a commercial processing environment, several modifications must be made. The design should be changed, or a filling method devised, such that filling the tubes with fluid becomes a simple, quick task. In addition, the sensor assemblies must be made more robust so that they can stand up to moderately rough handling and the force of the vacuum bag pulling on the sensor. For the instrumentation of large parts, many tube sensor assemblies would be required. To simplify the calibration stage of a large test, a single calibration equation for all of the sensors is desirable. Alternatively, the tube sensor assembly could be designed such that the sensors are easily reusable so that calibration would not have to be done for each test.

Most industrial cure cycles include temperatures of 180°C (350°F). The sensors used in this work have a maximum operating temperature of 125°C (260°F). Thus a higher temperature sensor must be used, or a method of insulating or cooling the sensors employed.

The detailed comparison of model and experiment has made it clear that it is difficult to accurately characterize prepreg. More experimental work is needed to determine the values of material parameters, such as the permeability of the fibre bed. It would also

be interesting to adjust the material parameters used in the simulation until the predicted resin pressure profile matches the experimental profile for the same laminate. This would lead to a better understanding of the effect of these material parameters on composite materials processing and perhaps to a closer estimate of their values.

Finally, the application of this work should not be limited to the autoclave vacuum degassing method described here as it would be equally suited to other composite processing methods such as hot press curing and resin transfer moulding.

References

[1] Purslow, D. & Childs, R., "Autoclave Moulding of Carbon Fibre-Reinforced Epoxies," *Composites*, Vol. 17, No. 2, 1986, pp. 127-136.

[2] Loos, A.C. & Freeman, W.T., "Resin Flow During Autoclave Cure of Graphite Epoxy Composites," in **High Modulus Fiber Composites in Ground Transportation and High Volume Applications, ASTM STP 873**, D.W. Wilson, Ed., American Society for Testing and Materials, 1985, pp. 119-130.

[3] Loos, A.C. & Springer, G.S., "Curing of Epoxy Matrix Composites," *Journal of Composite Materials*, Vol. 17, No. 2, March 1983, pp. 135-169.

[4] Gotro, J.T., Appelt, B.K. & Ellis, T.L., "Characterization of Resin Flow in Composites," Society of Plastics Engineers, 44th Annual Technical Conference, 1986, pp. 371-374.

[5] Skartsis, L., Khomami, B. & Kardos, J.L., "Resin Flow Through Fiber Beds During Composite Manufacturing Processes. Part II: Numerical and Experimental Studies of Newtonian Flow Through Ideal and Actual Fiber Beds," *Polymer Engineering and Science*, Vol. 32, No. 4, Feb. 1992, pp. 231-239.

[6] Poursartip, A., Riahi, G. & Smith, G., "Flow and Pressure Experiments for Laminate Fabrication," 36th International SAMPE Symposium, April 15-18, 1991, pp. 298-310.

[7] Poursartip, A., Riahi, G. & Smith, G., "Resin Flow During Autoclave Processing of Composite Laminates," 8th International Conference on Composite Materials, 1991, pp. 10-G-1 - 10-G-10.

[8] Poursartip, A., Riahi, G., Frederick, L. & Lin, X., "A Method to Determine Resin Flow During Curing of Composite Laminates," *Polymer Composites*, Vol.13, No.1, Feb. 1992, pp. 58-65.

[9] Cai, Z. & Gutowski, T., "Fiber Distribution and Resin Flow in the Laminate Molding Process," Proceedings of the Seventh International Conference on Composite Materials, Wu, V., Gu, Z. & Wu, R., Eds., Nov. 22-24, 1989, pp. 76-82.

[10] Smith, G.D., "Modelling and Experimental Issues in the Processing of Composite Laminates," MASc Thesis, University of British Columbia, Vancouver, August, 1992.

[11] MacKenzie, K.A., Smith, G.D. & Poursartip, A., unpublished results, 1991.

[12] Lindt, J.T., "Consolidation of Cylinders in Newtonian Fluid. I. Simple Cubic Configuration," *The Society of Rheology*, Vol. 30, No. 2, 1986, pp. 251-269.

[13] Lindt, J.T., "Engineering Principles of the Formation of Epoxy Resin Composites" Subtitle: "Mathematical Model of the Fluid Flow," *SAMPE Quarterly*, Vol. 14, Oct. 1982, pp. 14-19.

[14] Skartsis, L., Kardos, J.L. & Khomami, B., "Resin Flow Through Fiber Beds During Composite Manufacturing Processes. Part I: Review of Newtonian Flow Through Fiber Beds," *Polymer Engineering and Science*, Vol. 32, No. 4, Feb. 1992, pp. 221-230.

[15] Davé, R., Kardos, J.L. & Dudukovic, M.P., "A Model for Resin Flow During Composite Processing: Part 1 - General Mathematical Development," *Polymer Composites*, Vol. 8, No. 1, Feb. 1987, pp. 29-38.

[16] Springer, G.S., "Resin Flow During the Cure of Fiber Reinforced Composites," *Journal of Composite Materials*, Vol. 16, No. 5, Sept 1982, pp. 400-410.

[17] Davé, R., Kardos, J.L. & Dudukovic, M.P., "A Model for Resin Flow During Composite Processing: Part 2 - Numerical Analysis for Unidirectional Graphite/Epoxy Laminates," *Polymer Composites*, Vol. 8, No. 2, April 1987, pp. 123-132.

[18] Gutowski, T.G., "A Resin Flow/Fiber Deformation Model for Composites," *SAMPE Quarterly*, Vol. 16, No. 4, July 1985, pp. 58-64.

[19] Gutowski, T.G., Cai, Z., D., Kingery, J. & Wineman, S.J., "Resin Flow/Fiber Deformation Experiments," *SAMPE Quarterly*, Vol. 17, No. 4, 1986, pp. 54-58.

[20] Hou, T.H., "A Resin Flow Model for Composite Prepreg Lamination Process," Society of Plastic Engineers, Annual Technical Conference, 1986, pp. 1300-1305.

[21] Smith, G.D. & Poursartip, A., "A Comparison of Two Resin Flow Models For Laminate Processing," submitted to *Journal of Composite Materials*, Dec. 1992.

[22] Halpin, J.C., Kardos, J.L. & Dudukovic, M.P., "Processing Science: An Approach for Prepreg Composite Systems," *Pure and Appl. Chem.*, Vol. 55, No. 5, pp. 893-906, 1983.

[23] Roberts, R.W., "Controlling the Cure," in **Engineered Materials Handbook**, Volume 1, Dostral, C.A., Woods, M.S. & Ronke, A.W., Eds., ASM International, Ohio, U.S.A., 1987, pp.745-760.

[24] **Advanced Mechanics of Materials,** Fourth Edition, Boresi, A.P., Sidebottom, O.M., John Wiley & Sons, Inc., Toronto, 1932.

[25] **Marks' Standard Handbook for Mechanical Engineers**, Eighth Edition, T. Baumister, Ed., McGraw-Hill, 1978.

[26] Hercules Inc. Product Data Sheet 847-3, received from the manufacturer.

Appendix A: Displacement of the Tube Walls Due to Process Conditions

A.1. Hydrostatic Pressure

While the resin is fluid it exerts a hydrostatic pressure on the sensor tubing in the laminate. The length of tubing outside the vacuum bag experiences the hydrostatic autoclave pressure for the entire cure cycle. Radial displacement for an open, thick-walled, cylinder subjected to hydrostatic pressure, with no temperature changes, can be expressed [24] as follows:

$$u_{open\ end} = \frac{r}{E(b^2 - a^2)}\left[(1-\nu)(p_1 a^2 - p_2 b^2) + \frac{(1+\nu)a^2 b^2}{r^2}(p_1 - p_2)\right] \qquad \text{(A.1)}$$

where:

u	=	radial displacement
r	=	radial component
E	=	Young's modulus of the tube material
b	=	outside radius
a	=	inside radius
υ	=	Poisson's ratio
p_1	=	uniform internal pressure
p_2	=	uniform external pressure

For this case, the values used were as follows:

r	=	0.3048 mm
E	=	2.07×10^{11} Pa
b	=	0.5207 mm
a	=	0.3048 mm
υ	=	0.305

p_1 = 3.448 x 10^4 Pa (5 psia)
p_2 = 6.895 x 10^5 Pa (100 psia)

The result was a displacement of -1.079 x 10^{-6} mm.

A.2. Vertical Squeezing Pressure

After cure, the solid laminate applies a vertical force to the top and bottom of the sensor tubing. The resulting deflection of a thick-walled cylinder under these conditions is [25]:

$$\delta = \frac{1.5pd^4}{Et^3}\left\{\frac{\pi}{4} - \frac{2}{\pi}\right\} \qquad \text{(A.2)}$$

where:

δ = deflection of the tube wall
p = applied pressure
d = outside diameter
E = Young's modulus of the tube material
t = wall thickness

For this case, the values used were as follows:

p = 6.895 Pa
d = 1.067 x 10^{-3} m
E = 200 x 10^9 N
t = 1.905 x 10^{-4} m

The resulting deflection was found to be 0.143 μm. Another way of expressing this result is as a fraction of the diameter: δ/d. Expressed this way, the result is 0.01 %.

Appendix B: SenSym SCC100A Specifications

B.1. Pressure Sensor Characteristics

Maximum Ratings:

Supply Current, I_S	3.0 mA
Temperature Ranges:	
Compensated	0°C to +50°C
Operating	-40°C to +125°C
Storage	-55°C to +125°C
Humidity	0 to 100 % RH
Lead Temperature (soldering 10 sec)	300°C
Common-Mode Pressure	50 psi

B.2. Performance Characteristics

I_S = 1.5 mA, T_A = 25°C

Characteristics	Min.	Typ.	Max.	Unit
Zero Pressure Offset	-10.00	0.00	10.00	mV
Combined, Linearity, Hysteresis, Repeatability[1]	----	0.10	0.50	% FSO
Temperature Effect on Span [2]	----	0.25	1.50	% FSO
Temperature Effect on Offset [3]	----	0.50	2.00	% FSO
Long Term Stability of Offset and Span [4]	----	0.10	----	% FSO
Response Time (10% to 90%) [5]	----	0.10	----	mSec
Input Impedance	----	5.00	----	kΩ
Output Impedance	4.00	5.00	6.00	kΩ

Specification Notes:

1 Accuracy is the sum of Hysteresis and Linearity.

Hysteresis is the maximum output difference at any point within the operating pressure range for increasing and decreasing pressure.

Linearity refers to the best straight line fit as measured for the offset, full-scale and 1/2 full scale pressure.

2 This is the maximum temperature shift for span when measured between 0°C and 50°C relative to the 25°C reading.

Typical temperature coefficients for span and resistance are -2200 ppm/°C and +2200 ppm/°C respectively.

3 This is the maximum temperature shift for offset when measured between 0°C and 50°C relative to the 25°C reading.

4 Maximum difference in output at any pressure with the operating pressure range and temperature within 0°C and 50°C after:

a) 1,000 temperature cycles, 0°C and 50°C.

b) 1.5 million pressure cycles, 0 psi to full-scale span.

5 Response time for a 0 psi to full-scale span pressure step change, 10% to 90% rise time.

Appendix C: Nitric Acid Digestion of Laminates

The following procedure was used to determine the final volume fraction of fibres of the cured laminates. The nitric acid removes all resin from the fibres.

1. Weigh, and measure the volume of the composite sample.

2. Weigh filter paper (#42 ashless).

3. Place sample in excess boiling nitric acid.

4. Maintain boiling, stirring, for approximately 25 minutes.

5. Weigh backing paper.

6. Drain hot nitric acid and rinse remaining fibres: once with cold nitric acid, three times with water, and once with acetone.

7. Filter acetone and fibres.

8. Dry filter paper and fibres at 100°C overnight.

9. Weigh filter paper and fibres.

	Average Values for Each Test (g)		
	Laminate A	Laminate B	Laminate C
mass of composite sample	12.0243	26.834	10.6558
mass of filter paper	2.7158	2.7067	2.6614
mass of filter paper and fibres	11.4553	18.7289	9.9767

From the above data it is clear that:

	Values for Each Test (g)		
	Laminate A	Laminate B	Laminate C
mass of fibres	8.7395	16.0222	7.3153

and the mass fraction of fibres, M_f, can be found from the equation:

$$M_f = \frac{m_f}{m_c} \qquad \text{(C.1)}$$

where m_f is the fibre mass, and m_c the mass of the composite.

The density of the fibres, ρ_f, is 1.80 g/cm^3 [26]. Thus the volume fraction of fibres, V_f, of the laminate can be determined from the following equation.

$$V_f = \frac{\rho_c}{\rho_f} M_f \qquad \text{(C.2)}$$

The fibre volume fraction results for the three laminates are shown below.

	Laminate A	Laminate B	Laminate C
Average Volume Fraction of Fibres	0.614	0.491	0.596

Appendix D: Nitric Acid Digestion of Prepreg

The following procedure was used to determine the prepreg fibre volume fraction. The nitric acid removes all resin, cured or uncured, from the fibres. Unfortunately it will also attack the fibres: this is the reason for the fifteen minute limit.

1. Weigh, and measure the volume of the prepreg sample.

2. Weigh filter paper (#42 ashless).

3. Remove backing paper and place prepreg sample in excess nitric acid.

4. Heat nitric acid and prepreg, stirring, for 15 minutes.

5. Weigh backing paper.

6. Drain hot nitric acid and rinse remaining fibres: once with cold nitric acid, three times with water, and once with acetone.

7. Filter acetone and fibres.

8. Dry filter paper and fibres at 100°C overnight.

9. Weigh filter paper and fibres.

The measurements taken during the experiment are recorded below:

	mass (g)	average mass (g)
mass of prepreg and backing paper	16.9463, 16.9460	16.9462
mass of backing paper	4.7169, 4.7192	4.7181
mass of filter paper	2.7265, 2.7268	2.7267
mass of filter paper and fibres	9.6969, 9.7033, 9.7043, 9.7059	9.7026
mass of fibres	(9.7026 - 2.7267)	6.9759

The volume fraction of fibres of the prepreg can then be determined from the following equation:

$$V_f = \frac{\rho_c}{\rho_f} M_f \qquad \text{(D.1)}$$

where:

ρ_c = composite density
ρ_f = fibre density
M_f = mass fraction of fibres

The composite density is found from the mass of the composite, m_c, and its volume, Vol_c.

$$\rho_c = \frac{m_c}{Vol_c} \qquad \text{(D.2)}$$

The density of the fibres is provided by the manufacturer [24] as ρ_f=1.80 g/cm^3.
The mass fraction of fibres in the composite, is defined as follows:

$$M_f = \frac{m_f}{m_c} \qquad \text{(D.3)}$$

and the resin mass fraction is similarly:

$$M_r = \frac{m_r}{m_c} = 1 - M_f \qquad \text{(D.4)}$$

This data produced an average fibre volume fraction for the prepreg of 0.433, and a mass fraction of fibres of 0.57.

Appendix E: Input File For LamCure Simulations

[toolplateTemp]
298.76,305;
299.08,305;
299.45,70;
300.46,55;
301.52,45;
302.69,35;
303.94,40;
304.95,30;
305.96,30;
307.05,30;
308.1,30;
309.21,25;
310.32,25;
311.33,25;
312.45,25;
313.51,30;
314.66,30;
315.86,25;
316.96,30;
318.14,30;
319.23,25;
320.24,30;
321.45,30;
322.59,30;
323.88,30;
325.02,30;
326.19,25;
327.21,25;
328.22,30;
329.29,25;
330.4,30;
331.6,30;
332.76,30;
333.89,30;
335.02,25;
336.08,30;
337.19,30;
338.36,30;
339.52,25;
340.54,30;
341.66,30;
342.85,25;
343.86,30;
344.97,25;
346.02,30;
347.17,25;
348.19,30;
349.35,30;
350.46,25;
351.55,30;
352.68,30;
353.82,30;
354.99,30;
356.16,30;
357.32,30;
358.49,30;
359.66,30;
360.8,30;
362,30;
363.17,30;
364.4,30;
365.62,30;
366.72,30;
367.94,30;
369.16,30;
370.27,30;
371.4,25;
372.41,30;
373.61,30;
374.8,25;
375.84,30;
376.97,25;
377.98,30;
379.11,30;
380.32,30;
381.34,25;
382.36,25;
383.38,30;
384.53,30;
385.64,25;
386.78,30;
387.83,25;
388.92,30;
389.99,25;
391.06,30;
392.16,30;
393.34,25;
394.35,40;
395.44,305;
394.6,305;
393.91,300;
393.97,305;
393.91,305;
393.9,305;
393.92,305;
393.94,305;
394.01,305;
394.02,305;
394.06,305;
393.98,305;
394.02,305;
393.97,305;
394.03,305;
394.01,305;
393.94,305;
394.05,305;
394.05,305;
394.09,305;
394.07,305;
394.11,305;
394,305;
394.07,305;
394.1,305;
394.1,305;
394.09,305;
394.1,305;
394.06,305;
394.18,185;
393.2,5;

393.16,65;
392.06,70;
390.93,65;
389.9,45;
388.79,25;
387.66,30;
386.43,30;
385.34,30;
384.23,30;
383.22,30;
382.18,30;
381.1,35;
379.96,35;
378.81,35;
377.69,35;
376.62,35;
375.54,40;
374.41,40;
373.33,35;
372.29,50;
371.22,85;
370.13,200;
369.22,5;
368.37,15;
369.46,35;
370.47,105;
371.46,5;
371.48,305;
371.05,115;
370.11,5;
369.34,30;
370.48,305;
370.96,270;
370.1,5;
369.63,50;
370.64,305;
371.02,245;
370.19,5;
369.82,100;
370.82,5;
370.85,305;
371.06,145;
370.06,5;
369.44,100;
370.39,5;
370.47,65;
371.5,305;
371.83,130;
371.48,1;

[interfaceTemp]
298.76,305;
299.08,305;
299.45,70;
300.46,55;
301.52,45;
302.69,35;
303.94,40;
304.95,30;
305.96,30;
307.05,30;
308.1,30;
309.21,25;
310.32,25;
311.33,25;
312.45,25;
313.51,30;
314.66,30;
315.86,25;
316.96,30;
318.14,30;
319.23,25;
320.24,30;
321.45,30;
322.59,30;
323.88,30;
325.02,30;
326.19,25;
327.21,25;
328.22,30;
329.29,25;
330.4,30;
331.6,30;
332.76,30;
333.89,30;
335.02,25;
336.08,30;
337.19,30;
338.36,30;
339.52,25;
340.54,30;
341.66,30;
342.85,25;
343.86,30;
344.97,25;
346.02,30;
347.17,25;
348.19,30;
349.35,30;
350.46,25;
351.55,30;
352.68,30;
353.82,30;
354.99,30;
356.16,30;
357.32,30;
358.49,30;
359.66,30;
360.8,30;
362,30;
363.17,30;
364.4,30;
365.62,30;
366.72,30;
367.94,30;
369.16,30;
370.27,30;
371.4,25;
372.41,30;
373.61,30;
374.8,25;
375.84,30;
376.97,25;
377.98,30;
379.11,30;
380.32,30;
381.34,25;
382.36,25;
383.38,30;
384.53,30;
385.64,25;
386.78,30;
387.83,25;
388.92,30;
389.99,25;
391.06,30;
392.16,30;
393.34,25;
394.35,40;
395.44,305;
394.6,305;
393.91,300;
393.97,305;
393.91,305;

393.9,305;
393.92,305;
393.94,305;
394.01,305;
394.02,305;
394.06,305;
393.98,305;
394.02,305;
393.97,305;
394.03,305;
394.01,305;
393.94,305;
394.05,305;
394.05,305;
394.09,305;
394.07,305;
394.11,305;
394,305;
394.07,305;
394.1,305;
394.1,305;
394.09,305;
394.1,305;
394.06,305;
394.18,185;
393.2,5;
393.16,65;
392.06,70;
390.93,65;
389.9,45;
388.79,25;
387.66,30;
386.43,30;
385.34,30;
384.23,30;
383.22,30;
382.18,30;
381.1,35;
379.96,35;
378.81,35;
377.69,35;
376.62,35;
375.54,40;
374.41,40;
373.33,35;
372.29,50;
371.22,85;
370.13,200;
369.22,5;
368.37,15;
369.46,35;
370.47,105;
371.46,5;
371.48,305;
371.05,115;
370.11,5;
369.34,30;
370.48,305;
370.96,270;
370.1,5;
369.63,50;
370.64,305;
371.02,245;
370.19,5;
369.82,100;
370.82,5;
370.85,305;
371.06,145;
370.06,5;
369.44,100;
370.39,5;
370.47,65;
371.5,305;
371.83,130;
371.48,1;

[bleederTemp]
298.76,305;
299.08,305;
299.45,70;
300.46,55;
301.52,45;
302.69,35;
303.94,40;
304.95,30;
305.96,30;
307.05,30;
308.1,30;
309.21,25;
310.32,25;
311.33,25;
312.45,25;
313.51,30;
314.66,30;
315.86,25;
316.96,30;
318.14,30;
319.23,25;
320.24,30;
321.45,30;
322.59,30;
323.88,30;
325.02,30;
326.19,25;
327.21,25;
328.22,30;
329.29,25;
330.4,30;
331.6,30;
332.76,30;
333.89,30;
335.02,25;
336.08,30;
337.19,30;
338.36,30;
339.52,25;
340.54,30;
341.66,30;
342.85,25;
343.86,30;
344.97,25;
346.02,30;
347.17,25;
348.19,30;
349.35,30;
350.46,25;
351.55,30;
352.68,30;
353.82,30;
354.99,30;
356.16,30;
357.32,30;
358.49,30;
359.66,30;
360.8,30;
362,30;
363.17,30;
364.4,30;
365.62,30;
366.72,30;
367.94,30;
369.16,30;
370.27,30;
371.4,25;

372.41,30;
373.61,30;
374.8,25;
375.84,30;
376.97,25;
377.98,30;
379.11,30;
380.32,30;
381.34,25;
382.36,25;
383.38,30;
384.53,30;
385.64,25;
386.78,30;
387.83,25;
388.92,30;
389.99,25;
391.06,30;
392.16,30;
393.34,25;
394.35,40;
395.44,305;
394.6,305;
393.91,300;
393.97,305;
393.91,305;
393.9,305;
393.92,305;
393.94,305;
394.01,305;
394.02,305;
394.06,305;
393.98,305;
394.02,305;
393.97,305;
394.03,305;
394.01,305;
393.94,305;
394.05,305;
394.05,305;
394.09,305;
394.07,305;
394.11,305;
394,305;
394.07,305;
394.1,305;
394.1,305;
394.09,305;
394.1,305;
394.06,305;
394.18,185;
393.2,5;
393.16,65;
392.06,70;
390.93,65;
389.9,45;
388.79,25;
387.66,30;
386.43,30;
385.34,30;
384.23,30;
383.22,30;
382.18,30;
381.1,35;
379.96,35;
378.81,35;
377.69,35;
376.62,35;
375.54,40;
374.41,40;
373.33,35;
372.29,50;
371.22,85;
370.13,200;
369.22,5;
368.37,15;
369.46,35;
370.47,105;
371.46,5;
371.48,305;
371.05,115;
370.11,5;
369.34,30;
370.48,305;
370.96,270;
370.1,5;
369.63,50;
370.64,305;
371.02,245;
370.19,5;
369.82,100;
370.82,5;
370.85,305;
371.06,145;
370.06,5;
369.44,100;
370.39,5;
370.47,65;
371.5,305;
371.83,130;
371.48,1;

[vacuumPressure]
4809.062545,305;
4809.062545,305;
4809.062545,305;
4809.062545,305;
4809.062545,305;
4809.062545,305;
4809.062545,305;
4809.062545,305;
4809.062545,305;
4809.062545,305;
4809.062545,305;
4809.062545,305;
4809.062545,305;
4809.062545,272.2;
4964.4,0;
3115.72639,642.8;
3115.72639,305;
3115.72639,305;
3115.72639,305;
3115.72639,305;
3115.72639,305;
3115.72639,300;
3115.72639,305;
3309.6,-4;
1422.39713,614;
1422.39713,305;
1422.39713,305;
1422.39713,305;
1422.39713,305;
1422.39713,305;
1422.39713,305;
1422.39713,305;
1422.39713,305;
1422.39713,305;
1422.39713,305;
1422.39713,305;
1422.39713,629;
1422.39713,0;
5516,108;
5516,0;
1422.39713,788;
1422.39713,305;
1422.39713,305;
1422.39713,594;
1422.39713,16;
6502.391805,152;
6619.2,24;
4809.062545,239;
4964.4,5;
20225.427565,10;
33179.45708,10;
44064.44189,10;
53210.85245,10;
60896.37799,10;
101328.92,230;
101328.92,1;

[externalPressure]
103195.8102,305;
103185.12295,305;
103111.76015,30;
111486.70295,5;
122932.6098,5;
136781.631,5;
152386.395,5;
169077.811,5;
187934.9465,5;
203442.491,5;
217444.1675,5;
232778.6475,5;
250900.0865,5;
268689.876,5;
286239.7195,5;
305661.5555,5;
321508.334,5;
341094.271,5;
357145.831,5;
374238.536,5;
391276.081,5;
407906.821,5;
427447.251,5;
442988.581,5;
462591.066,5;
479518.291,5;
498141.686,5;
516647.866,5;
534540.391,5;
554487.626,5;
570104.800999999,5;
589369.431,5;
604283.316,5;
620734.786,5;
636551.915999999,5;
652431.101,5;
668868.781,5;
681969.281,15;
691408.536,7.8;
708088.92,16.2;
704779.32,111;
695897.181,110;
689250.400999999,5;

688416.106,110;
703124.52,249;
689403.47,108;
693816.27,146.4;
693816.27,184.2;
687403.92,135.6;
695953.72,102.6;
696643.22,169.2;
688024.47,128.4;
693126.77,395.4;
690575.62,178.8;
696367.42,108.6;
688713.97,93.8;
691705.021,202;
688507.12,408;
696850.07,60;
688423.001,60;
680962.611,50.4;
675475.57,114.6;
688360.946,87;
698229.07,88;
688636.746,5;
688229.941,60;
681010.876,120;
687774.871,5;
688278.206,145;
694807.771,5;
695738.596,300;
688905.651,5;
688788.436,369.2;
690491.501,240.8;
696448.781,55;
689215.926,55;
682231.290999999,60;
674943.276,10;
685266.47,59.2;
678233.57,155.8;
690201.911,85;
697172.755999999,43;
699883.87,567;
693021.966,305;
691408.536,305;
691187.896,503;
690753.511,310.8;
695195.27,101.2;
687912.771,305;
693980.371,138;
693402.57,204;
688024.47,573;
690029.535999999,305;
690912.095999999,305;
691429.221,305;
691353.376,354;
691015.520999999,211;
697876.046,107;
700780.22,158;
691263.741,5;
690870.725999999,155;
684106.731,5;
683968.831,145;
690484.606,81.6;
693402.57,93.4;
684734.175999999,21.2;
680095.22,13.8;
693228.816,60;
686195.916,55;
679280.231,116.6;
665684.67,13.4;
687437.016,90.4;
693807.996,196.2;
694781.57,311.4;
687541.82,190.8;
682922.17,185.4;
697332.72,92.4;
696643.22,43.8;
694092.07,158.4;
696160.57,146.2;
693816.27,5;
657429.976,5;
602711.256,5;
550833.276,5;
536650.261,5;
520984.821,140;
514317.356,5;
513931.236,95;
507374.091,5;
506705.276,305;
507236.191,20;
463963.171,5;
420690.151,5;
387849.266,5;
378382.431,305;
381540.341,285;
382815.916,5;
351967.686,5;
322050.281,5;
294787.451,5;
268157.582,5;
248061.415,205;
241247.776,5;
241080.2275,305;
246157.7055,60.8;
244055.42,9.2;
217068.39,5;
198342.2595,5;
184275.77,5;
169339.1315,5;
158143.0305,5;

147176.533,5;
137624.8895,5;
129292.9715,5;
121551.955,10;
110788.86,15;
102683.2359,215;
101544.044,5;
110771.8983,5;
124999.455,5;
141328.194,5;
154897.554,5;
170668.4875,5;
186016.068,5;
201019.588,5;
216649.8635,5;
229440.0885,5;
244467.741,5;
256536.0595,5;
269265.6085,5;
281595.937,5;
293646.3285,5;
306506.193,5;
316887.305,5;
328950.1075,5;
338763.761,5;
349113.156,5;
359152.276,5;
368694.956,5;
378720.286,5;
387766.526,5;
396619.706,5;
404342.106,5;
412464.416,5;
420138.551,5;
428060.906,5;
435776.411,13.4;
447959.876,117;
437804.92,4.6;
394240.931,5;
357552.636,5;
330007.111,5;
300193.131,5;
277237.6075,5;
254770.25,5;
233901.843,5;
215465.3025,5;
197076.3375,5;
183163.6065,5;
168446.9185,5;
157384.5805,5;
145668.5965,5;
137158.7875,5;
128911.678,5;
121236.164,10;
110663.371,15;
102706.74785,305;
101374.63385,205;
101469.23325,1;

[timeStep]
15, 1199;
15, 1;
60, 20940;

[voidRatioVsFiberPressur
e]
1.06781,68928.57;
0.703612,34464.23;
0.660117,34464.3;
0.629257,34464.3;
0.605321,34464.3;
0.585763,34464.3;
0.569227,34464.2;
0.554903,34464.3;
0.542268,34464.3;
0.530966,34464.3;
0.520742,34464.3;
0.511408,34464.3;
0.502822,34464.3;
0.494872,34464.2;
0.487471,34464.3;
0.480548,34464.3;
0.474045,34464.3;
0.467913,34464.3;
0.462114,34464.3;
0.456611,34464.3;
0.451378,34464.2;
0.446387,34464.3;
0.441619,34464.3;
0.437054,34464.3;
0.432675,34464.3;
0.428467,34464.3;
0.424419,34464.3;
0.420518,34464.2;
0.416753,34463.8;
0.413117,1;

```
[execution]
parallelFlow=false;
perpendicularFlow=true;
flowModel=sponge;
mixing=laminar;
checkDiagonalDominance=true;
permeabilityModel=variable;
thermalModel=calculate;

[bleeder]
GenBleeder, 0.1016, 0.1016, 5.6e-11, 0.57;

[fiber]
GenFibers, 1799.0, 0.721, 26.0e-3, 26.0e-3, 8.4e-6;

[resin]
GenThermoset, 1220.0, 1.26, 1.67e-4, 474.0, 80.7, 77.8, 56.6, 90.8, 3.5017e7, -
3.3567e7, 3.2667e3, 7.93e-14, 0.47, 14.1, 0.3;

[laminate]
48, 0.1016, 0.1016, 0.00271, 0.42, false, false, false, circular, 0, 298.76;

[fileOutput]
{c:\akathy\0c4norm.opt}
printEvery=60;
bleeder= resinHeight;
laminate= viscosity, avg, fiberVolumeFraction, avg, degreeOfCure, avg;
lamina= resinPressure, 0, interfaceResinPressure, 11, interfaceResinPressure, 23,
interfaceResinPressure, 35, interfaceResinPressure, 47, fiberPressure, 0,
fiberPressure, 11, fiberPressure, 23, fiberPressure, 35, fiberPressure ,47, voidRatio, 0,
voidRatio, 11, voidRatio, 23, voidRatio, 35, voidRatio, 47;

[end]
```

Appendix F: Acetone Digestion of Prepreg

The following procedure was used to determine the cured resin mass fraction in the prepreg. The acetone removes all uncured resin from the fibres, leaving the cured resin.

1. Weigh the prepreg sample.

2. Weigh filter paper (#42 ashless).

3. Remove backing paper and place prepreg sample in excess acetone.

4. Heat acetone and prepreg, stirring, for at least 30 minutes.

5. Weigh backing paper.

6. Filter acetone and fibres.

7. Rinse well, several times, with acetone, stirring fibres to separate them.

8. Dry filter paper and fibres at 100°C overnight.

9. Weigh filter paper and fibres.

This procedure was done to three pieces of prepreg; the results follow:

	Average Values for Each of Three Tests (g)		
	Sample #1	Sample #2	Sample #3
mass of prepreg and backing paper	16.419	16.296	16.344
mass of backing paper	4.652	4.766	4.738
mass of filter paper	2.762	1.151	1.119
mass of filter paper and filtrate	10.269	8.367	8.285

From the above data it is clear that:

	Values for Each of Three Tests (g)		
	Sample #1	Sample #2	Sample #3
mass of prepreg	11.767	11.530	11.606
mass of filtrate	7.507	7.216	7.166

The mass of the fibres, m_f, is found from the mass fraction of fibres of the prepreg, M_f, found in Appendix D, and the mass of the prepreg used, m_c, for each sample.

$$m_f = M_f m_c \qquad \text{(F.1)}$$

The cured resin mass, m_{cr}, is the filtrate mass, m_{filt}, less the mass of the fibres.

$$m_{cr} = m_{filt} - m_f \qquad \text{(F.2)}$$

The total mass of resin, m_r, is found in a similar way to the mass of the fibres.

$$m_r = M_r m_c \qquad \text{(F.3)}$$

The cured resin mass fraction in the prepreg, R, is then found as follows:

$$R = \frac{m_{cr}}{m_r} \qquad \text{(F.4)}$$

	Values for Each of Three Tests			
	Sample #1	Sample #2	Sample #3	Average
R	0.158	0.130	0.110	0.133

The average cured resin mass fraction of the prepreg, from the three samples, was 0.133.

Appendix G: Conversion of Resin Height in the Bleeder to Resin Mass

The value for resin height in the bleeder, output from LamCure, can be converted to a resin mass in the bleeder, by the following expression.

$$mass = resin\,density \times occupied\,volume\,of\,bleeder \times bleeder\,porosity \qquad \text{(G.1)}$$

The occupied volume of the bleeder is the resin height, multiplied by the area of the bleeder, 103.226 cm^2. The porosity of the bleeder used by LamCure is 0.57 and the density of the resin is 1.22 g/cm^3.

The results for the varying degrees of cure considered are shown below.

Initial Degree of Cure	Final Resin Height (m)	Occupied Volume of Bleeder (cm^3)	Final Resin Mass (g)
0	0.00436	45.01	31.297
0.05	0.00436	45.01	31.297
0.10	0.00436	45.01	31.297
0.15	0.00436	45.01	31.297
0.20	0.00432	44.59	31.010
0.25	0.00381	39.33	27.349
0.30	0.00214	22.09	15.362
0.35	0.00157	16.21	11.270

Appendix H: Resin Mass Lost from Laminates A and C

In this appendix, the amount of resin lost from Laminates A and C are calculated in two ways. First, the difference in the mass of the bleeder plies before and after the cure cycles are measured. If all resin that leaves a laminate enters and remains in the bleeder, then this technique will produce the mass of the resin lost from the laminate. The second method determines, from experimental measurements of the mass and area of prepreg and laminate samples, the mass per area ratio of the prepreg and the cured laminates. From these ratios, the amount of mass lost per area and per laminate can be caluculated. The results of the mass change/area method are checked by using these results to predict the total prepreg mass using the separately measured mass fraction of fibres of the laminates and the prepreg. The results are very similar. Finally, in Section H.4, the results of the bleeder mass method and mass change per area method are compared and shown to agree well.

H.1. Bleeder Masses

Comparing the initial and final masses of the bleeder plies for Laminates A and C, results in the mass of resin in the bleeder for each case.

	mass of bleeder layers (g)		resin mass in bleeder (g) (calculated)
	initial	final	
Laminate A	24.95	49.57	24.62*
Laminate C	36.34	55.27**	18.93

* some resin spilled out of the bleeder layers during cure, so this value may be low

** the lower bleeder tube was locked in the resin, so its estimated mass of 0.365 g was subtracted from the measured mass

H.2. Mass Change per Area

The resin mass lost from a laminate during cure can be determined from the mass change per area from the prepreg to the laminate.

From the prepreg it can be found that, for one ply:

	mass (g)	area (cm^2)	mass/area (g/cm^2)
Prepreg	11.767	451.5	0.0261

The mass/area on a per ply basis for Laminates A and C can be calculated from pieces of the laminates, as follows:

	mass (g)	area (cm^2)	laminate mass/area (g/cm^2)	per ply mass/area (g/cm^2)
Laminate A	12.0243	12.36	0.973	0.0203
Laminate C	10.6558	10.08	1.058	0.0220

The mass of resin lost for a laminate, per ply, per cm^2, can then be found by subtracting the mass/area of the cured laminate from the mass/area of the prepreg.

$$mass\,loss\,per\,ply = {}^{mass}/_{area}\,of\,prepreg - {}^{mass}/_{area}\,of\,laminate \qquad \text{(H.1)}$$

Then, over the whole laminate,

$$mass\,loss = area \times \#\,plies \times mass\,loss\,per\,ply \qquad \text{(H.2)}$$

	area (cm^2)	# plies	per ply mass loss per ply (g/cm^2)	laminate mass loss (g)
Laminate A	103.23	48	0.0058	28.738
Laminate C	103.23	48	0.0041	20.315

H.3. Checking the Mass Change per Area Results With the Measured Laminate and Prepreg M_f Results

The resin lost from the laminate determined from the mass change per area can be checked by using the, experimentally determined, resin mass fractions of the prepreg, and the cured laminates.

The mass of the prepreg laminates was:

Laminate A 130.12 g
Laminate C 129.56 g

Using the mass losses calculated by the mass change per area results, the final masses of the two laminates should be:

Laminate A 101.38 g
Laminate C 109.25 g

The mass fraction of fibres, M_f, of each laminate was determined by nitric acid digestion (described in Appendix C). The fibre mass of each laminate can then be determined from the equation:

$$fibre\ mass = M_f \times composite\ mass \qquad \text{(H.3)}$$

and the resin mass is the mass which remains.

$$resin\ mass = composite\ mass - fibre\ mass \qquad \text{(H.4)}$$

So final properties of Laminates A and C should be,

	Experimental	Calculated From Mass/Area Results		
	M_f	composite mass	fibre mass	resin mass
Laminate A	0.7268	101.38 g	73.68 g	27.70 g
Laminate C	0.6865	109.25 g	75.00 g	34.25 g

If the resin loss masses calculated from the mass loss/area method are now added to the resin masses in the table above, the result should be the total amount of resin in the prepreg. The resin mass fraction of the prepreg was experimentally determined (Appendix D) to be 0.43, and can be used to convert the prepreg resin mass to a total mass of the prepreg laminate. This can then be compared to the measured total prepreg mass, to determine the validity of the mass loss per area method.

	Calculated From Mass/Area Results				Experimental
	final resin mass	resin mass lost	total prepreg resin mass	total prepreg mass	total prepreg mass
Laminate A	27.70 g	28.738 g	56.44 g	131.26 g	130.12 g
Laminate C	34.25 g	20.315 g	54.57 g	126.91 g	129.56 g

The results are very similar for both laminates. The mass change/area results will now be compared with the bleeder mass results.

H.4. Comparison of Bleeder Mass and Mass Change per Area Results

	total resin mass loss (g)	
Technique	Bleeder Mass	Mass Change per Area
Laminate A	24.62	28.738
Laminate C	18.93	20.315

The results for the two methods are similar with differences of 14.3 % for Laminate A and 6.8 % for Laminate C. The bleeder mass results are lower, which is expected since not all of the resin resides in the bleeder after cure. The mass change per area method considers the change in the laminate directly, but relies on accurate measurement of representative areas of prepreg and composite samples. In Laminate A, some resin had overflowed from the bleeder layers which explains the larger difference in the results from the two methods for this laminate.